WORKING PAPERS

N° 1622

March 2025

"Climate Change, Labor Market Frictions, and Inequality"

Aditya Goenka, Lin Liu, Manh-Hung Nguyen and Haokun Pang

Toulouse School of Economics

Climate Change, Labor Market Frictions, and Inequality

Aditya Goenka*
University of Birmingham

Lin Liu†
University of Liverpool

Manh-Hung Nguyen‡
Toulouse School of Economics

Haokun Pang§
Imperial College London

March 6, 2025

Abstract

We model the impact of rising temperatures on labor productivity, labor market dynamics, and income inequality. Using a heterogeneous agent continuous-time (HACT) model with directed search, we analyze how temperature-induced productivity fluctuations influence the labor market, income and wealth inequality, and wealth accumulation. The model features workers differentiated by wealth, productivity, and location, where temperature affects transitions between high and low productivity states. Firms post fixed-wage contracts, and workers direct their job search across segmented labor markets. We calibrate the model using Vietnamese Labor Force data (2009-2018) matched with meteorological records, capturing regional temperature variations. With increased temperatures, in low wage markets the ratio of vacancies to unemployed workers searching in those market falls, as labor productivity declines and falling wealth leads workers to direct their search to these markets when vacancies are also falling. The wage distribution shifts to the left, and average incomes and wealth fall. Climate-induced productivity shocks amplify income and wealth disparities as wealthier individuals are able to self-insure better against the income risk. The results underscore the role of climate change in shaping labor market inequality and provide insights into policy interventions that may mitigate its adverse effects.

Keywords: *Climate change, HACT model, Directed search, Income inequality*
JEL Classification: *Q54, J64, J23, J31, E24, C64*

*Department of Economics, University of Birmingham, Email: a.goenka@bham.ac.uk

†Management School, University of Liverpool, Email: lin.liu@liverpool.ac.uk

‡Toulouse School of Economics, INRAE, University of Toulouse Capitole, Toulouse, France. Email: manh-hung.nguyen@tse-fr.eu. Manh-Hung Nguyen acknowledges funding from ANR under grant ANR-17-EURE-0010 (Investissements d'Avenir program) and from the Sophie Germain program, funded by the French Ministry for Europe and Foreign Affairs (MEAE), the Embassy of France in the United Kingdom, and the French Ministry of Higher Education and Research (MESR).

§Business School, Imperial College London, Email: h.pang@imperial.ac.uk.

I. Introduction

Global warming, driven by rising greenhouse gas emissions, has led to a steady increase in global temperatures over the past century. According to the IPCC, global average surface temperature has risen by approximately 1.1°C since the late 19th century, with projections indicating further warming of 1.5–4.5°C by 2100 depending on emission scenarios. The developing economies are especially vulnerable to climate change.The effects of this temperature increase on economic systems are receiving increasing attention. A growing body of research has highlighted its effects on economic productivity. These effects vary across sectors, income groups, and regions. How this impacts economic inequality within an economy is not well understood as yet. This paper develops a heterogeneous agent continuous time (HACT) model with labor market frictions to study the effects of increases in temperature on worker productivity, labor market dynamics, and income inequality. We use Vietnamese Labor Force and matched meteorological data to calibrate the data.

Rising temperatures can affect labor productivity via two channels: First, absenteeism due to physiological exhaustion or sickness can decrease the extensive margin of the labor force (Zander et al. (2015)). Besides health impacts, the marginal cost of supplying labor increases under high temperatures that can shift time allocation preferences of workers towards valuing leisure time more than paid working hours (Graff Zivin and Neidell, 2014). Second, poor cognitive performance and physiological stress at work - for instance, due to the lack of climate control - can decrease the intensive margin of labor productivity by reducing individual efficiency (Garg, Jagnani and Taraz (2020), Zhang, Chen and Zhang (2024), Zivin et al. (2020)). At the macroeconomic level, Dell, Jones and Olken (2012) show that higher temperatures reduce GDP growth in low-income countries by 1.3% per 1 °C increase, while having negligible effects on wealthier economies. This disparity underscores the vulnerability of developing nations, which rely heavily on temperature-sensitive sectors such as agriculture and low-skill manufacturing. Burke, Hsiang and Miguel (2015) further refine this relationship, showing that economic productivity follows a non-linear inverted U-shape response to temperature. The peaks vary across regions and type of activity and declining sharply beyond this threshold. At the sectoral level, studies provide micro-level evidence on the mechanisms driving these productivity losses. Somanathan et al. (2021) analyze Indian manufacturing firms and find that a 1°C increase in temperature reduces annual factory output by 2%, primarily due to lower worker efficiency and increased absenteeism. Similar patterns are observed in Graff Zivin and Neidell (2014), who show that on hot days above 29.5 °C, outdoor workers in the U.S. reduce their work hours by up to one hour per day, with limited evidence of short-run adaptation. Zhang et al. (2018) find that both

labor- and capital-intensive Chinese manufacturing firms suffer productivity losses during extreme heat, suggesting that temperature effects extend beyond human labor to machine efficiency and industrial workflows. In addition to labor-intensive sectors, cognitive performance is also affected, as studies show that students and professionals perform worse on tasks requiring analytical reasoning in high-heat conditions (Carleton and Hsiang (2016)) Despite some evidence that abatement (air conditioning and technological improvements) can mitigate productivity losses, these adaptations come at significant economic and environmental costs, particularly in developing countries where access to cooling infrastructure remains limited. These studies highlight that rising temperatures can reduce economic productivity.

The differential impairment of productivity can lead to widening of inequalities across countries. Dell, Jones and Olken (2012) similarly find that higher temperatures reduce GDP growth in low-income countries while having little to no effect on wealthier economies, suggesting that climate change exacerbates global economic divergence. Diffenbaugh and Burke (2019)) estimate that climate change has already widened the income gap between the richest and poorest countries due to differential growth effects.

However, there can also be effects on inequalities within countries. The mechanisms and estimates of how inequality changes due to temperature within a country are not fully explored and understood (see Dang, Nguyen and Trinh (2023), and Dang, Hallegatte and Trinh (2024)) even though low-income workers, particularly those in outdoor and labor-intensive jobs, face greater productivity losses and income volatility due to heat exposure (Graff Zivin and Neidell (2014), Somanathan et al. (2021)).

In this paper we develop a HACT model (Achdou et al. (2022), Huggett (1993)) with labor market frictions similar to the competitive directed search model (Chaumont and Shi (2022), Krusell, Luo and Rios-Rull (2023)). Krusell and Smith Jr (2022) use a neoclassical representative agent model but here as we want to model inequalities we use a HACT framework. In the model, workers are heterogenous indexed by their productivity, wealth, and the location they work in. Productivity can either by high or low and is private knowledge to the worker and is revealed to the employer only after a successful match. Based on their location they are affected by temperature changes which can cause a change in productivity, with higher temperatures increasing the probability of transiting from a high to low productivity. Individuals can save in an asset with a no-borrowing constraint. As the evidence suggests that temperature abatement plays a small role for worker productivity we do not model it. Workers can either be employed or unemployed. An employed worker is separated from the job exogenously. Firms post vacancies which is a non-negotiable wage and unemployed workers direct their search to a sub-market. They

become employed depending on the market tightness which is the ratio of vacancies to workers looking for jobs in that sub-market. Firms enter the sub-market until profits are zero. In Chaumont and Shi (2022) the firms can observe the wealth of the worker and make wage offers contingent on the wealth levels. We assume that wealth is not observable as in Krusell, Luo and Rios-Rull (2023), though in equilibrium individual wealth will influence which sub-market the worker will search in. The take-home pay of the worker depends on the contracted wage times the productivity. An unemployed worker in addition to the consumption-savings choice has to choose which sub-market to search in. The wealth level acts as partial insurance mechanism as there are no contingent claims markets to insure against all risk. Where we differ from these papers (Chaumont and Shi (2022)), Krusell, Luo and Rios-Rull (2023), Eeckhout and Sepahsalari (2024)) is in making the changes in productivity depend on changes in temperature thus, making the labor market interact with climate change.[1] To quantify these effects, we estimate the productivity transition probabilities using empirical data and map them into a continuous-time Poisson framework. We characterize the policy functions of the workers, calculate the stationary equilibrium, and conduct comparative dynamic analysis to see how changes in temperature will affect the labor market and the inequality in income and wealth.

The relationship between temperature and productivity is based on the Vietnam Labor Force data (2009-2018) and meteorological data from the Vietnam Institute of Meteorology, Hydrology, and Climate Change, covering temperature and precipitation records from 172 weather stations nationwide.[2]. The Vietnamese Labor Force data has indicators for a worker including location. Thus, we can match the two data sets to study how changes in temperature affects a given worker's productivity. This matched data is used to calibrate the transition probabilities between the high and low productivty as dependent on temperatures. The data on productivity is consistent with the Burke, Hsiang and Miguel (2015) finding that the relationship between productivity and temperature is an inverted U-shape.

We find that temperature fluctuations have pronounced non-linear effects on labor market behavior, altering both firms' hiring decisions and workers' job search strategies. In particular, equilibrium market tightness, defined as ratio of vacancies to unemployed workers searching in that market, exhibits an inverse U-shaped relationship with temperature. Starting from cooler conditions, a rise in temperature initially increases market tightness - reflecting more vacancies per job seeker – but beyond a threshold this trend reverses: Extreme heat induces firms to antic-

[1] In the model, we make a small-open economy assumption as in Chaumont and Shi (2022) and keep the interest rate fixed so that there is no capital income risk as in Benhabib, Bisin and Zhu (2015).

[2] See discussion of these data sets in Section 2

ipate productivity losses and cut back on vacancy postings, resulting in a tighter job market (fewer openings relative to unemployed workers) at high temperatures. As a result, unemployment risk rises once temperatures exceed the productivity-optimum range. Importantly, this impact is heterogeneous across job types: high-wage jobs are less sensitive to temperature variation, showing smaller declines in vacancy rates than low-wage jobs. On the worker side, rising temperatures initially encourage unemployed individuals to search for higher-paying jobs (as long as labor market conditions remain favorable), but beyond a certain heat threshold their optimal search wage begins to decline. In other words, when faced with heat-driven job scarcity, job seekers become more risk-averse and target lower-wage positions to improve their chances of employment. This adjustment is especially pronounced for asset-constrained workers: poorer individuals are less selective and tend to seek low-wage jobs under high-temperature stress, whereas wealthier job seekers can afford to hold out for better-paying opportunities. These findings underscore a critical employment dynamic – moderate warming can temporarily loosen the labor market, but severe heat ultimately tightens market conditions, shifts job searches downward along the wage ladder, and raises the likelihood of unemployment. In the model there are two kinds of risks that workers face: the risk that productivity will change and the risk of not finding a job when unemployed. The first is partially insured by accumulating savings, and the second by searching for a lower paying job where they are relatively more vacancies per job.

At the aggregate level, the model predicts that sustained increases in temperature will depress overall economic outcomes while amplifying disparities. The equilibrium wage distribution shifts to the left and broadens under warmer climates, indicating a greater prevalence of low-wage work and increased wage dispersion as temperatures rise. Accordingly, the unemployment rate climbs with warming. Our simulations show a clear upward trend in unemployment as average temperature increases, with especially sharp upticks once average temperatures exceed roughly 28°C. These labor market effects translate into lower aggregate income and wealth and a more unequal economy. For example, in a scenario where the average temperature rises from about 25°C to 30.5°C (consistent with end-of-century climate projections for Vietnam), mean income falls by roughly 1.4% and mean wealth by about 1.0%, even as the income Gini index increases by about 0.7% and the wealth Gini by about 0.3%. In general, income inequality worsens monotonically with temperature: higher average heat exposure leads to a higher income Gini coefficient, a pattern that is even more pronounced when the distribution of temperatures skews toward extreme heat (e.g. under a right-tailed temperature distribution). Wealth inequality exhibits a somewhat U-shaped response – it initially narrows at mild warming (as households deploy precautionary savings to buffer income shocks) but widens once

temperature rises become extreme. The slower change in wealth inequality is due to workers partially self-insuring against productivity risk by accumulating savings and against unemployment risk by searching in lower wage markets. Richer workers are more choosy in which jobs they will accept - higher paying jobs - as well as they decrease their marginal propensity to consumer by more than less well off workers to better insure against the productivity risk. Climate scenarios with more frequent extreme-temperature days exacerbate all of these trends: a greater share of the population exposed to severe heat further tightens the labor market and magnifies the increases in unemployment and inequality. Overall, both the empirical estimation and calibrated simulations indicates that rising temperatures can erode employment opportunities and wage gains while intensifying economic inequality, with the adverse effects accelerating as the climate grows hotter.

The structure of the paper is organized as follows: section II. introduces the main dataset used in this study and motivates our structural model by presenting key empirical findings. section III. then outlines the theoretical model, including its setup and equilibrium conditions. In section IV., we describe how the model is calibrated using our empirical data. Next, section V. and section VI. present the main results and predictions derived from the model. Finally, section VII. provides concluding remarks.

II. Empirical Motivation

This paper studies the effect of climate change on productivity in Vietnam. Vietnam is considered a country that is extremely vulnerable to climate change. It has a population of about 100 million making it the 15th largest country in the world. It is located in the South-East Asia on the eastern margin of the Indochinese peninsula with an area of is about 331,211.6 square kilometres (127,881.5 sq mi). It has an elongated roughly S shape with a north-to-south distance of 1,650 km (1,030 mi) and is about 50 km (31 mi) wide at the narrowest point. The country is a mix of subtropical and tropical lowlands, hills, and densely forested highlands, with level land covering less than 20% of the area. The coastline of the country is 3,260 km (2,030 mi) and 70% of the population resides in the coastal region.

Vietnam is located in the tropics and it has a monsoon influenced climate as other South-East Asian countries. The country spans 15°of the latitude and this is reflected in the climate. The north has a humid sub-tropical and monsoonal climate (four seasons) while the central and southern regions of the country is typical tropical monsoonal climate (two seasons – wet and dry). The highlands have a more temperate and continental climate. The national average daily temperature is approximately 25 °C, with the mean annual temperature ranging from 12.8 to

27.7 °C (55 to 82 °F) across the country. The mountainous areas, as altitude is higher, and the northern regions, as latitude is higher, have the lowest mean annual temperatures . The warmest parts of the year are March-May in the south and May-July in the north. Temperatures in summer are relatively similar between the northern and southern parts of the country, and the differences largely due to altitude.

The annual temperature nationwide have increased by 0.89°C between 1958-2018 (about 0.15 °C per decade). The largest increase was in 2008-2018. Annual rainfall has also increased by 5.5% on average. There are spatial variations in the change in temperature and rainfall, with temperature expected to rise faster in the north than in the south of the country. The projections for the increase in temperature range by the end of the 21st century range from 1.13 ± 0.87°C to 4.18 ± 1.57°C depending on the different global scenarios for greenhouse gas emissions. Rainfall is also expected to increase in Vietnam but with a different seasonal pattern (See Espagne et al. (2021) for details on climate change projections.)

A. The Data

We analyze data from Vietnam's Labor Force Survey (LFS), conducted annually by the General Statistics Office (GSO) from 2009 to 2018. The LFS is the primary source of official labor statistics in Vietnam, employing a two-stage stratified cluster sampling approach that ensures national representativeness at the provincial and urban/rural levels. Each year, the sample is evenly distributed, with approximately one-twelfth of selected households surveyed monthly. The surveys collect comprehensive labor market data, including hourly earnings, employment status, industry, education, and demographic characteristics for individuals aged 15 and older.

To ensure our results are unaffected by pandemic-related disruptions, we use only pre-COVID-19 data. In 2018, Vietnam's labor force participation rate was 76.7%, with 82.1% for males and 71.6% for females. Despite ongoing urbanization, 67.8% of the labor force remained in rural areas, where participation was higher (81.6%) compared to urban areas (68.2%). Sectoral employment shares in 2018 were 38.6% in agriculture, forestry, and fishery, 26.5% in industry and construction, and 34.8% in services. The unemployment rate was relatively low at 2.2%, while an additional 1.6% were underemployed, working fewer than 35 hours per week but available for additional work.[3] Our analysis is based on more than 1.5 million observations from the 2009-2018 period.

The second dataset comprises climate data from the Vietnam Institute of Meteorology, Hydrology, and Climate Change, covering temperature and precipitation

[3]These statistics are from 2018 LFS, Office (2018).

records from 172 weather stations nationwide. To integrate these datasets, each district is matched with the nearest weather station based on the shortest centroid-to-station distance. The meteorological stations collect daily temperature readings, and we calculate the average daily temperature for each year to derive the yearly temperature. Each district is assigned a temperature value based on calculations that consider the distances from four nearby weather stations, with weights applied according to the shortest centroid-to-station distance. As a result, all individuals within the same district share the same temperature value. There are approximately 700 districts in the country, and the temperature varies across districts and years (See Nguyen, Nguyen and Nguyen (2023) for further details). Given the available meteorological data, all districts in a given province are assigned the same temperature, which we account for using fixed effects. These climate data are then merged with the LFS data for analysis.

B. Empirical Specification and Results

For each individual i in district ω during year t, the temperature is denoted as $T_{\omega t}$. To analyze the determinants of wages, we estimate the following fixed effects regression model which studies the effect of temperature on log hourly wages. The models incorporate individual, location, and time-fixed effects to ensure robust estimation and mitigate potential omitted variable bias. Previous literature has documented the adverse effects of extreme temperatures on labor productivity. However, the relationship between temperature and wages is not necessarily linear.

$$\begin{aligned}\ln(Wage_{i,\omega,t}) = \alpha_1 \text{Age}_{i,\omega,t} + \alpha_2 \text{Edu}_{i,\omega,t} + \alpha_3 \text{Male}_{i,\omega,t} + \alpha_4 \text{Occupation}_{i,\omega,t} \\ + \alpha_5 T_{\omega,t} + \alpha_6 T^2_{\omega,t} + \gamma_i + \gamma_\omega + \gamma_t + \epsilon_{i,\omega,t}\end{aligned} \tag{1}$$

where $\ln(Wage_{i,\omega,t})$ represents the logarithm of the hourly wage for individual i in district ω at year t, $\text{Age}_{i,\omega,t}$ denotes the age of individual i, $\text{Edu}_{i,\omega,t}$ is a dummy variable indicating whether the individual has vocational education (1 if yes, 0 otherwise), $\text{Male}_{i,\omega,t}$ is a gender dummy variable (1 if male, 0 if female), $\text{Occupation}_{i,\omega,t}$ represents the occupation category of individual i, $\text{Industry}_{i,\omega,t}$ denotes the industry category in which the individual is employed, γ_i captures individual fixed effects to control for time-invariant unobserved individual characteristics, γ_ω represents fixed location effects to account for geographic differences, γ_t includes fixed effects in time

Table I. Regression Results: Impact of Temperature on Wages

Variable	Estimate	Std. Error
Avg. Temperature	0.04292***	0.009432
Avg. Temp Squared	-0.000627**	0.000194
Age	0.0000343***	0.0000083
Education (Vocational)	0.111426***	0.002066
Gender (Male)	0.153299***	0.001772
Occupation	-4.86e-18**	1.72e-18
Industry	0.130058***	0.001447
Observations	1,507,718	
RMSE	0.5801	
Adjusted R^2	0.2524	
Within R^2	0.0586	

Notes: This table presents the regression results examining the relationship between temperature and wages. Standard errors are clustered at the individual level. Statistical significance: $^{*}p < 0.10$, $^{**}p < 0.05$, $^{***}p < 0.01$.

to control for macroeconomic trends and time-specific shocks, $\epsilon_{i,\omega,t}$ is the error term.[4]

Our regression results provide insight into how temperature fluctuations affect wages. Table I presents the estimated coefficients for temperature-related variables. The coefficient on average temperature is positive and statistically significant, indicating that within a certain range higher temperatures are associated with increased wages. This suggests that economic activity in warmer regions might benefit from industrial and service-sector expansion.

However, the quadratic term for temperature is negative and statistically significant, confirming a concave inverted U-shaped relationship. This implies that while wages initially rise with temperature, they begin to decline at very high temperatures, likely due to adverse productivity effects, health risks, and work environment challenges. Other control variables, including education, gender, occupation, and industry effects, exhibit expected patterns. Education remains a strong predictor of wage increases, with vocational training contributing to higher earnings. Males earn significantly more than females, highlighting persistent gender wage disparities.

The regional differences in temperature and income also highlight the complex relationship between climate and economic activity. In Vietnam, for example, the South experiences hotter temperatures yet has higher average incomes compared to the North. This disparity suggests that factors beyond temperature alone—such as

[4]Following the literature, we also construct several bins for temperature. The value for each bin is the number of days in a year that daily temperature falls into the category. We then regress log wage on the value of bins for all categories in addition to all other controls and fixed effects. We find similar results, that is, individuals experiencing more days with high temperature have lower wage.

industrial composition, labor market structures, and economic policies—contribute to income levels. In hotter regions, workers may transit to more heat-adapted industries such as manufacturing and services, where wages tend to be higher. Moreover, urbanization and investment in climate resilience can mitigate some of the adverse productivity effects of high temperatures.

To further illustrate the distribution of temperatures across Vietnam, we provide a heatmap in Figure 1. The figure demonstrates clear differences in temperature across regions, with the North experiencing colder climates and the South exhibiting significantly higher temperatures. These climatic variations correspond to differences in income levels and economic structures, further supporting the argument that temperature influences wage levels and productivity transitions.

Figure 1. Annual Temperature Distribution in Vietnam for 2009 and 2018. Source: 172 Weather Stations.

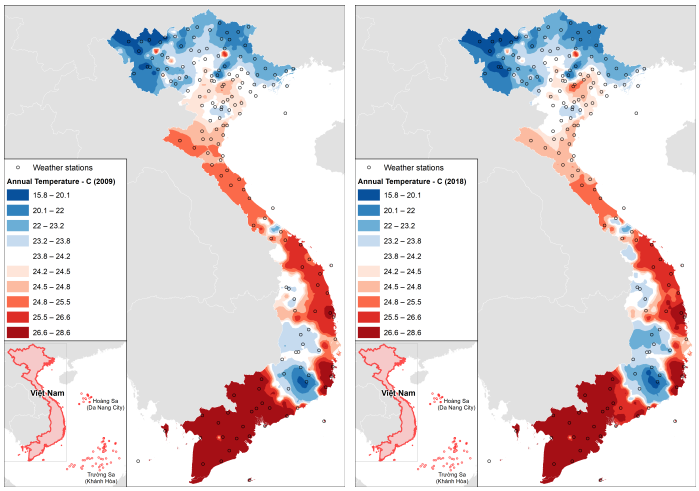

(a) Temperature Distribution in 2009 **(b)** Temperature Distribution in 2018

Notes: (a) This figure depicts the annual temperature distribution in Vietnam for the years 2009 (Panel a) and 2018 (Panel b), based on data from 172 weather stations. (b) The color gradient represents temperature variations, with blue shades indicating lower temperatures and red shades indicating higher temperatures.

Figure 2 illustrates the distribution of average temperatures across Vietnam. The distribution exhibits two distinct peaks, corresponding to the country's two major climatic regions. The northern region experiences a wider temperature range, including lower temperatures, while the southern region, which is generally hotter, contributes to the higher-temperature peak. The overall shape suggests a right-skewed distribution, characteristic of a Log-normal distribution. The presence of two main peaks indicates bimodality, likely driven by seasonal and geographical variations between the cooler North and the hotter South. The empirical distribution can be approximated using a bimodal distribution with either normal components

Figure 2. Temperature distribution

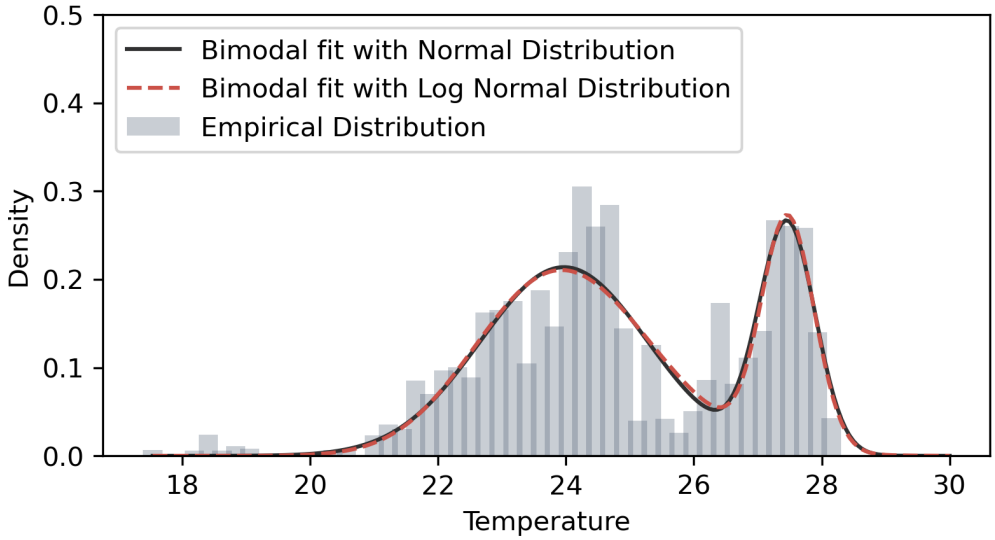

Notes: (a) This figure compares the empirical temperature distribution (gray bars) with two fitted bimodal distributions. (b) The black solid line represents the Bimodal fit using Normal distributions, while the red dashed line represents the Bimodal fit using Lognormal distributions.

(Bimodal-Normal) or log-normal components (Bimodal-Log-normal). We will introduce this bimodal approximation in more detail in section IV.. As a preview, we plot the Bimodal fits using solid and dashed lines. It can be observed that both Bimodal distributions fit the empirical data well, with only a small difference in their goodness of fit.

III. The Model

This paper develops a searching and matching model in a heterogeneous-agent, continuous-time framework (Achdou et al., 2022). Specifically, we extend the Huggett-Bewley model by incorporating direct search *à la* Chaumont and Shi (2022) and the increase in temperature due climate change affecting labor productivity. Time, indexed by t, is continuous. The economy consists of infinitely lived, individuals with heterogeneity along multiple dimensions. The labor market includes jobs that are either filled or vacant. A representative firm hires workers, while unemployed individuals search for jobs. Individuals can save in an asset that pays a rate of return, r. We make the small-open economy assumption so that the determination of r is not modelled.

A. Labor Market and Climate

In the labor market, unemployed workers search for jobs, and firms divide the market into multiple sub-markets where they post vacancies. In a given sub-market, let u and v denote the number of unemployed workers and vacancies, respectively. Market tightness is defined as $\theta = \frac{v}{u}$, where lower values indicate a tighter market. Assuming that the matching function $\mathcal{M}(u, v)$ is homogeneous of degree 1, the job-finding rate j and the vacancy-filling rate f are given by

$$j(\theta) = \frac{\mathcal{M}(u,v)}{u} = \frac{v}{u}\mathcal{M}\left(\frac{u}{v}, 1\right) = \theta\mathcal{M}\left(\frac{1}{\theta}, 1\right), \tag{2}$$

$$f(\theta) = \frac{\mathcal{M}(u,v)}{v} = \mathcal{M}\left(\frac{u}{v}, 1\right) = \mathcal{M}\left(\frac{1}{\theta}, 1\right), \tag{3}$$

where in equilibrium, market tightness θ is endogenous and varies across submarkets. We will later introduce how firms segment the job market.

To model climate change, we focus on temperature, denoted by T. We assume that T is heterogeneous that individuals work in the workplace with different temperatures consistent with the spatial variation in Vietnam. As detailed later, we assume T directly affects workers' productivity. The temperature in the workplace is potentially affected by exogenous variations in temperature, global warming, and workplace conditions. For simplicity we abstract from temperature abatement measures, treating T as exogenous meaning individuals and firms take it as given when optimizing their behavior.

B. Individual Workers

Productivity: We assume that workers can have two productivity levels, $z \in \{z_1, z_2\}$, where $z_2 > z_1$. Productivity evolves stochastically according to a two-state Poisson process. The transition probabilities depend on the temperature an individual is exposed to. Specifically, for workers working under temperature T, the transition intensities are given by

$$\lambda_T(z) = \begin{cases} \pi_1(T), & z = z_1, \\ \pi_2(T), & z = z_2, \end{cases} \tag{4}$$

where π_1 denotes the transition intensity from low to high productivity, and π_2 denotes the transition intensity from high to low productivity. In the following section on estimation and calibration, we estimate the functional form of the transition intensity using the Labor Force Survey in Vietnam. We assume that the productivity is match-specific, unobservable during the job search process, and realized

ex-post after employment. Consequently, firms' hiring strategies do not depend on productivity z.

Employment Status: The economy consists of a pool of heterogeneous jobs, indexed by the contracted real wage rate $w \in \mathcal{W}$. Individuals are either employed ($q = 1$) or unemployed ($q = 0$). Employed workers earn labor income equal to their contracted wage rate multiplied by productivity, i.e., wz. Jobs have a fixed term and are subject to an exogenous destruction rate ξ. Unemployed workers do not earn labor income and search for jobs. They aim to find the best available job by selecting which job, characterized by wage w, to target in their search. If a worker searches in a specific submarket, the probability of a successful match is $j(\theta(w))$, where $\theta(w)$ represents the market tightness for that submarket. For simplicity, we assume no search costs or unemployment benefits, as is the case in Vietnam.

Wealth Accumulation: Both employed and unemployed workers hold assets $a \in [\underline{a}, \bar{a}]$, which evolve according to

$$\dot{a} = ra + wz\mathbb{1}(q = 1) - c, \tag{5}$$

where r is the real interest rate and c is consumption. Under the small open economy assumption, r is exogenously given.

Optimization Problem: Individuals maximize their expected lifetime utility, given by

$$\mathbb{E}\int_0^\infty e^{-\rho t}u(c)dt, \tag{6}$$

where ρ is the discount factor and $u(c)$ is the twice continuously differentiable strictly concave utility function. There is a no-borrowing constraint so that $a \geq \underline{a}$.

The model incorporates heterogeneity in three dimensions: (match-specific) productivity z, employment status q, and wealth a. Among employed workers, heterogeneity extends to the contracted wage rate w. The temperature, T is a state-variable and it affects the decision problem of individuals in several ways: it affects the possible transition of their current match-specific productivity when employed, and for the unemployed affects their choice of which sub-market to search as the firms decide how many vacancies to post in each sub-market, thus, affecting the market tightness condition. The value functions for employed and unemployed workers for a given temperature, T are denoted as $E_T(a, z, w)$ and $U_T(a, z)$, respectively. Their corresponding Hamilton-Jacobi-Bellman (HJB) equations are:

$$\begin{aligned}\rho E_T(a,z,w) = \max_{c} \quad & u(c) + \frac{\partial E_T}{\partial a}(ra + wz - c) \\ & + \lambda_T(z)[E_T(z',a,w) - E_T(a,z,w)] \\ & + \xi[U_T(a,z) - E_T(a,z,w)] + \frac{\partial E_T}{\partial t},\end{aligned} \tag{7}$$

$$\begin{aligned}\rho U_T(a,z) = \max_{c,w} \quad & u(c) + \frac{\partial U_T}{\partial a}(ra - c) \\ & + \lambda_T(z)[U_T(z',a) - U_T(a,z)] \\ & + j(\theta(w))[E_T(a,z,w) - U_T(a,z)] + \frac{\partial U_T}{\partial t}.\end{aligned} \tag{8}$$

We can derive the optimal conditions for individuals as:

$$\begin{aligned} c^* &= \begin{cases} u'^{-1}\left(\frac{\partial E_T}{\partial a}\right), & q = 1, \\ u'^{-1}\left(\frac{\partial U_T}{\partial a}\right), & q = 0, \end{cases} \\ w^* &= \arg\max_{w} \quad j(\theta(w))[E_T(a,z,w) - U_T(a,z)]. \end{aligned} \tag{9}$$

Note, that the problem is a concave problem and the sufficient first order conditions for the consumption-savings choice which depend only on wealth level which is the asset holdings, a, can be inverted to yield the policy functions as in Equation 9. The choice of which wage to target by an unemployed worker will depend on their current productivity level and their wealth level. Furthermore, let $g_T^E(a,z,w)$ and $g_T^U(a,z)$ denote the joint distributions of employed and unemployed workers, respectively. The evolution of these distributions follows the Kolmogorov Forward Equations:

$$\begin{aligned}\dot{g}_T^E(a,z,w) = & -\frac{\partial}{\partial a}[\dot{a} g_T^E(a,z,w)] - \lambda_T(z) g_T^E(a,z,w) + \lambda_T(z') g_T^E(z',a,w) \\ & - \xi g_T^E(a,z,w) + \mathbb{1}(w^* = w) j(\theta(w)) g_T^U(a,z),\end{aligned} \tag{10}$$

$$\begin{aligned}\dot{g}_T^U(a,z) = & -\frac{\partial}{\partial a}[\dot{a} g_T^U(a,z)] - \lambda_T(z) g_T^U(a,z) + \lambda_T(z') g_T^U(z',a) \\ & - \sum_w j(\theta(w)) g_T^U(a,z,w) + \sum_w \xi g_T^E(a,z,w).\end{aligned} \tag{11}$$

The Kolmogorov Forward Equations represent the change in the joint distribution of the state variables. The first, Equation 10 shows that it changes due to the change in asset holdings, flow out of the given productivity due to temperature, flow into that productivity due to the temperature, loss of jobs due to exogenous separations and the new matches created. The second, Equation 11 has the same first three terms and the last two terms are the exit due to new matches and entry due of

exogenous separations.

C. *Production Landscape*

The production landscape consists of multiple jobs that differ in wage rates. Jobs can be either filled or vacant. If a job with wage w is filled by a worker of productivity z, its instantaneous profit is given by $\Pi(z, w) = y(z) - wz$. Since productivity evolves stochastically and employment contracts are subject to destruction, the Hamilton-Jacobi-Bellman (HJB) equations for jobs, denoted by $J_T(z, w)$ is given by

$$\begin{aligned} \rho^{\mathtt{f}} J_T(z,w) =& \Pi(z,w) + \xi[V - J_T(z,w)] \\ &+ \lambda_T(z)[J_T(z',w) - J_T(z,w)] + \frac{\partial J_T}{\partial t}, \end{aligned} \tag{12}$$

where $\rho^{\mathtt{f}}$ is the firm's discount rate, equal to the real interest rate plus capital depreciation, $r + \delta$. The value of a filled job is affected by the job destruction probability, $\xi[V - J_T(z, w)]$, and by workers' productivity transitions, $\lambda_T(z)[J_T(z', w) - J_T(z, w)]$. Similarly, the value of a vacancy satisfies the following HJB equation:

$$\rho^{\mathtt{f}} V = -\kappa + f(\theta(w))[J_T(z,w) - V] + \frac{\partial V}{\partial t}, \tag{13}$$

where κ is the cost of posting a vacancy, $f(\theta(w))$ is the vacancy-filling rate, and the term $f(\theta(w))[J_T(z, w) - V]$ captures the expected change in value when a vacancy is filled by a worker of productivity z, and wage w. Note that the productivity of a worker becomes observable to the firm only after a vacancy is filled. Thus, the firm in evaluating the value of a vacancy conditions on the temperature, T, as this influences the distribution of productivity of workers.

D. *Equilibrium Conditions*

Firms hire workers by posting vacancies to target market tightness $\theta(w)$. In equilibrium, tightness satisfies the free-entry condition, ensuring that the value of a vacancy V in Equation 13 is always zero. This implies $\kappa = f(\theta(w))J_T(z, w)$.

However, we assume that the labor market features incomplete information: match-specific productivity z is unobservable during the job search process. Firms must investigate the job market and infer the expected productivity for the unemployed individuals. We further assume that firm could obtain the conditional distribution of productivity given temperature in the job market, i.e. $\mathbb{P}(z|T, q = 0)$. Consequently, the free-entry condition is specified using the conditional expectation:

$$\kappa = f(\theta(w))\mathbb{E}[J_T(z,w)|T, q = 0]. \tag{14}$$

This implies that equilibrium market tightness is a function temperature and wage rate, as given by Equation 15:

$$\theta_T(w) = f^{-1}\left(\frac{\kappa}{\mathbb{E}[J_T(z,w)|T, q=0]}\right). \tag{15}$$

This paper focuses on the stationary equilibrium of the model, defined as follows:

Definition 1. *Given the real interest rate r, for each under temperature T, an equilibrium consists of individual value functions (E_T, U_T), firm value functions $J_T(z,w)$, individual distributions (g_T^E, g_T^U), and equilibrium market tightness $\theta_T(w)$ such that:*

1. *$\{(E_T, U_T)\}_t$ solve the individuals' HJB equations (Equation 7, Equation 8), taking market tightness $\theta_T(w)$ as given.*
2. *$J_T(z,w)$ solves the jobs' HJB equation (Equation 12).*
3. *The joint distribution (g_T^E, g_T^U) evolves according to the Kolmogorov Forward Equations (Equation 10, Equation 11).*
4. *The value functions and distributions are stationary, meaning they do not change over time:*

$$\frac{\partial E_T}{\partial t} = \frac{\partial U_T}{\partial t} = \frac{\partial J_T}{\partial t} = \frac{\partial g_T^E}{\partial t} = \frac{\partial g_T^U}{\partial t} = 0.$$

5. *The equilibrium market tightness $\theta_{i,T}(w)$ satisfies the free-entry condition (Equation 15).*

Thus, as in Chaumont and Shi (2022) an small open-economy assumption is made so that the interest rate determination is not modelled.

We solve this model using the Finite Differencing Method (FDM), following the approach in Achdou et al. (2022). A detailed description of the solution method and algorithm is provided in Appendix C.

IV. Estimation and Calibration

A. *Estimating the Productivity Transition*

In our model, a key functional component is the transition intensity between the high-productivity and low-productivity states. In this section, we estimate this transition using the Vietnamese data introduced in section II. We follow a standard two-stage approach as outlined below:

(Step 1) Estimating Productivity: In the first step, we estimate Equation 16.[5] This specification is similar to Equation 1, except that we exclude the

[5]The notation for variables in this section follows the conventions introduced in section II.

temperature variables T_{wt}. In this setup, temperature-related effects are absorbed into the error term $\epsilon_{i,\omega,t}$. This approach aligns with our structural model's assumption that temperature does not directly influence workers' wages but instead affects them indirectly through unobservable productivity channels.

$$\begin{aligned}\ln(Wage_{i,\omega,t}) = \beta_1 \text{Age}_{i,\omega,t} + \beta_2 \text{Edu}_{i,\omega,t} + \beta_3 \text{Male}_{i,\omega,t} + \beta_4 \text{Occupation}_{i,\omega,t} \\ + \gamma_i + \gamma_\omega + \gamma_t + \epsilon_{i,\omega,t}.\end{aligned} \tag{16}$$

The regression is estimated using a fixed-effects OLS approach. The estimated residual term $\varepsilon_{i,\omega,t}$ captures unobserved productivity factors that are not accounted for by the included explanatory variables. These unobservable components may include individual-specific abilities, motivation, work ethic, or other external environmental factors influencing productivity. Since individual and location fixed effects control for systematic differences across people and places, the residual variation primarily reflects productivity fluctuations due to unobserved short-term shocks, firm-level dynamics, and measurement errors.

To ensure consistency with our structural model, which assumes a binary productivity state, we classify continuous productivity estimates into either a high or low level. We define $P_{i,\omega,t} \in \{H, L\}$ to represent the empirical productivity state. As a classification threshold, we use the statistical mean of the estimated residuals, $\bar{\varepsilon}$, which is approximately zero in practice. Individuals with residuals above the mean ($\varepsilon_{i,\omega,t} > \bar{\varepsilon}$) are assigned to the high-productivity group ($P_{i,\omega,t} = H$), while those with residuals below the mean ($\varepsilon_{i,\omega,t} < \bar{\varepsilon}$) are assigned to the low-productivity group ($P_{i,\omega,t} = L$). This classification approach enables us to proxy unobserved heterogeneity in productivity levels and analyze how external factors, such as temperature and precipitation, influence transitions between these two productivity states.

(Step 2) Estimating the Transition Probabilities: To estimate the transition probabilities, we first calculate two transitional indicators. We define a binary variable $D_{i,\omega,t}^{L\to H}$, which equals 1 if $P_{i,\omega,t} = L$ and $P_{i,\omega,t+1} = H$, indicating individuals who transition from a low-productivity state at time t to a high-productivity state at time $t+1$. Individuals with $D_{i,\omega,t}^{L\to H} = 0$ remain in the low-productivity state. Conversely, we define another binary variable, $D_{i,\omega,t}^{H\to L} = 1$, to indicate individuals whose productivity declines from a high state to a low state, i.e., those with $P_{i,\omega,t} = H$ and $P_{i,\omega,t+1} = L$.

Finally, we use Equation 17 to evaluate the effect of temperature on productivity transitions, where the explained variable $\mathbf{D}_{i,\omega,t}$ includes both the indicator for low-to-high transition ($D_{i,\omega,t}^{L\to H}$) and high-to-low transition ($D_{i,\omega,t}^{H\to L}$). In this specification, we focus on the marginal effects of average temperature by including a second-order polynomial term, $T_{\omega,t}$ and $T_{\omega,t}^2$, in the explanatory variables. We also control for

precipitation ($\text{Pre}_{\omega,t}$) as a standard approach for empirical research on climate.

$$\mathbf{D}_{i,\omega,t} = \beta_0 + \beta_1 T_{\omega,t} + \beta_2 T_{\omega,t}^2 + \beta_3 \text{Pre}_{\omega,t} + v_{i,\omega,t}. \tag{17}$$

Given the binary explanatory variables, we estimate Equation 17 using a Generalized Linear Model (GLM) with a binomial Logit specification. Table II presents the results of the logit regression estimates showing the transition probabilities for productivity low to high and productivity high to low, respectively.

Table II. Logistic Regression Results

	High to Low		Low to High	
Variable	Estimate	Std. Error	Estimate	Std. Error
Intercept	-1.0668***	0.2226	-2.2037***	0.2256
Avg. Temperature	-0.0208	0.0182	0.0669***	0.0184
Precipitation	1.6e-5***	3.3e-6	2.5e-5***	3.3e-6
Avg. Temp Squared	0.0005	0.0004	-0.0012**	0.0004
Observations	1,507,718		1,507,718	
Log-Likelihood	-799,737.3		-799,429.1	
Adjusted Pseudo R^2	1.89e-5		7.47e-5	
BIC	1,599,531.6		1,598,915.0	
Squared Correlation	2.41e-5		8.31e-5	

Notes: This table presents the results of logistic regressions estimating the probability of transitioning between productivity states. Standard errors are reported in parentheses. Statistical significance: $^*p < 0.10$, $^{**}p < 0.05$, $^{***}p < 0.01$.

We now describe how we map the regression results to the transition matrix. Since we use the Logit function as the link function in the GLM, the coefficients in Equation 17 measure the marginal effects of the explanatory variables on the log-odds ratio of transition. We transform the log-odds ratio into transition probabilities as follows:

$$\begin{aligned} \mathbb{P}(P_{i,\omega,t+1} = L | P_{i,\omega,t} = H) &= \text{Logit}(\hat{D}_{\omega,t}^{L\to H}) \equiv \mathcal{F}_1(T, \text{Pre}), \\ \mathbb{P}(P_{i,\omega,t+1} = H | P_{i,\omega,t} = L) &= \text{Logit}(\hat{D}_{\omega,t}^{H\to L}) \equiv \mathcal{F}_2(T, \text{Pre}), \end{aligned} \tag{18}$$

where $\text{Logit}(x) = \frac{e^x}{1+e^x}$ is the link function, and $\hat{D}_{\omega,t}^{L\to H}$ and $\hat{D}_{\omega,t}^{H\to L}$ are the fitted values from the regressions under given temperature and precipitation conditions. By defining $\mathcal{F}_1(T, \text{Pre})$ as the probability of transitioning from low to high productivity and $\mathcal{F}_2(T, \text{Pre})$ as the probability of transitioning from high to low productivity, given temperature and precipitation, we express the Markov transition matrix as:

$$\mathcal{T}(T, \text{Pre}) = \begin{bmatrix} 1 - \mathcal{F}_1(T, \text{Pre}) & \mathcal{F}_1(T, \text{Pre}) \\ \mathcal{F}_2(T, \text{Pre}) & 1 - \mathcal{F}_2(T, \text{Pre}) \end{bmatrix}. \tag{19}$$

Linking the Estimation to the Structural Model: In this paper, our empirical data from Vietnam is of annual frequency, while our model follows a continuous-time setup. To reconcile this difference, we transform the discrete-time Markov transition matrix into a continuous-time Poisson process by solving for the generator matrix Q, which satisfies:

$$\mathcal{T}(T, \text{Pre}) = e^{Q(T,\text{Pre})\Delta t}, \tag{20}$$

where Δt represents the time step in the continuous-time model. In linking this to our model in section III., we abstract from the effect of precipitation and fix precipitation, Pre, at its mean level from the dataset, i.e., 1973 mm per year. Consequently, the transition intensities, $\pi_1(T)$ and $\pi_2(T)$ in Equation 4, correspond to the off-diagonal elements of the generator matrix.

To illustrate how productivity changes with temperature in our estimation, we solve for stationary productivity given $T \in [10, 50]$ and plot the corresponding results as a solid line in Panel (a) of Figure 3. As a reference, we also include a red dashed line, obtained by following the same procedure but modifying the first-stage regression in Equation 16 to control only for time fixed effects γ_t and district fixed effects γ_w. The difference in stationary productivity between these two specifications is minimal. Therefore, in our subsequent analysis, we focus only on results where individual fixed effects are controlled for.

Examining the pattern in Figure 3, we observe a clear inverse U-shaped relationship between stationary productivity and temperature. This finding is consistent with the results presented earlier in section II.. When temperature is below a certain threshold, higher temperatures are associated with increased productivity. However, as the average temperature continues to rise, average productivity declines correspondingly.

B. Other Calibrations

Distribution for Average Temperature: In our model, the distribution for temperature state, i.e. $\mathbb{P}(T)$ is also requiring. In the shown in Figure 2, the empirical distribution in our data shows characteristic of bimodality. Therefore, we fit the empirical temperature distribution using a bimodal distribution with different specifications, as defined in Equation 21 and Equation 22, where we use a Normal distribution ($\mathcal{N}(\mu, \sigma^2)$) and a Log-normal distribution ($\text{LogN}(\mu, s)$) as the respective components. For simplicity, we refer to these as the Bimodal-Normal distribution and Bimodal-Log-normal distribution in our subsequent analysis. We present the corresponding parameter estimation results in Table A1 and plot the fitted values in blue solid and red dashed lines in Figure 2. Both the Bimodal-Normal and Bimodal-

Figure 3. Stationary Productivity and Marginal Effects

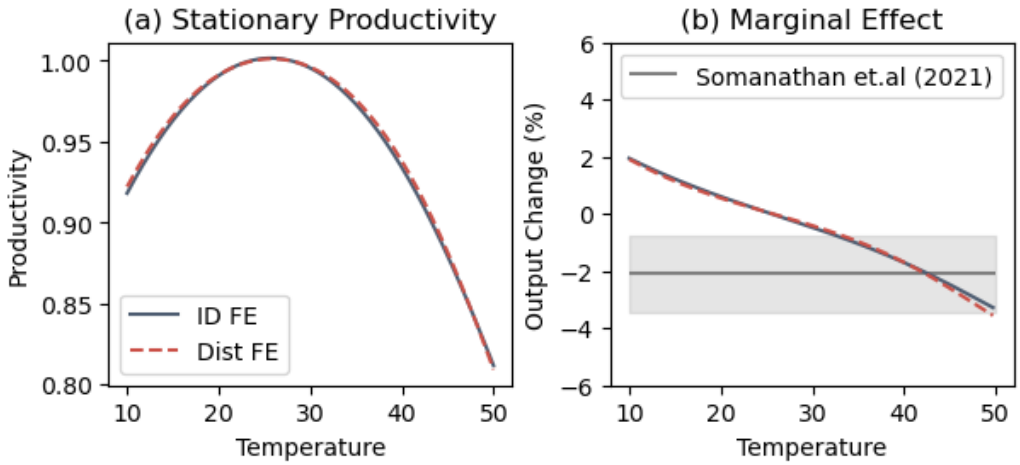

Notes: (a) Panel (a) shows stationary productivity as a function of temperature. It is obtained by computing the stationary distribution given the transition intensities $\{\pi_1(T), \pi_2(T)\}$, which are estimated from empirical data. (b) The solid and dashed lines represent results from estimations using individual fixed effects (ID FE) and district fixed effects (Dist FE), respectively. (c) Panel (b) illustrates the marginal effect of temperature on output change (%). The black line represents the estimates from Somanathan et al. (2021), with the shaded region indicating the 90% confidence interval.

Log-normal distributions fit the empirical data well, with only a small difference in their goodness of fit.

$$\mathbb{P}(T) = p_1 \mathcal{N}(\mu_1, \sigma_1^2) + p_2 \mathcal{N}(\mu_2, \sigma_2^2), \tag{21}$$

$$\mathbb{P}(T) = p_1 \text{LogN}(\mu_1, \sigma_1^2) + p_2 \text{LogN}(\mu_2, \sigma_2^2). \tag{22}$$

Parameterization: The remaining parameters in the model are calibrated in a standard way. We calibrate the model to a seasonal frequency. For the lifetime utility function, we calibrate the CES utility function as $u(c) = \frac{c^{1-\varrho}}{1-\varrho}$ with $\varrho = 2$ and set the subjective discount rate to $\rho = 0.0138$.

Regarding the parameters for the labor market, we first specify the matching function $\mathcal{M}(u, v)$. Various functional forms have been suggested in the literature; in this paper, we assume a Cobb-Douglas form, $\mathcal{M}(u, v) = u^{\varpi} v^{1-\varpi}$. We set the parameter $\varpi = 0.68$ so that the elasticity of the job-finding rate with respect to market tightness θ is 0.32, consistent with the values in Chaumont and Shi (2022); Eeckhout and Sepahsalari (2024). Second, we calibrate the job destruction rate to $\xi = 0.085$, implying a 3-year average contract duration. Third, for the firm's search cost κ, we calibrate this parameter to target the unemployment rate. We set $\kappa = 0.1$, which results in a generated unemployment rate of approximately 4.5% to 5%,[6] as

[6]This is consistent with the unemployment + underemployment rate of about 4% in Vietnam.

we will demonstrate in subsequent sections.

For the production function $y(z)$ and the real interest rate r, since they are directly correlated with individuals' labor and capital income, we calibrate them to match the average capital income share. We first set $r = 0.012$, which corresponds to an annual percentage rate (APR) of 4.8%. Then, we assume a functional form $y(z) = z^{\alpha}$ and calibrate $\alpha = 2$ so that the capital income share in total income is approximately 25%.

We summarize the calibration in Table III. To further validate our parameterization, we compute the average output $\mathbb{E}[y(z)]$ under various temperature levels. Next, we calculate the marginal change in average output when temperature increases by 1°C. The results are depicted in Panel (b) of Figure 3. It can be observed that the marginal effect on output is negative and decreases when the average temperature exceeds a certain threshold. The predicted marginal effect closely aligns with the estimate by Somanathan et al. (2021) when $T > 30°C$, which is approximately -2.1, with a 90% confidence interval of $[-0.75, 3.45]$.

Table III. Parameterization

Parameter	Interpretation	Target	Value
$\pi_1(T)$, $\pi_2(T)$	Transition intensity functions for productivity	Estimated from empirical data	–
ϖ	Elasticity parameter in the Cobb-Douglas matching function $\mathcal{M}(u,v) = u^{\varpi}v^{1-\varpi}$	Job-finding rate elasticity of market tightness ≈ 0.32	0.68
ξ	Job destruction rate	Average contract duration of 3 years	0.085
κ	Search cost	Unemployment rate between 4% and 6%	0.1
α	Output elasticity in the production function $y(z) = z^{\alpha}$	75% of the labor income share	2
r	Real interest rate	4.8% APR	0.012

Notes: This table presents the functions and parameters used in this paper. The function of transition intensities are estimated from the empirical data. The rest of the parameters are calibrated.

V. The Effects of Temperature on Labor Market Behaviors

We now present the main empirical results of our paper. We begin with evaluating how firms' optimal hiring strategies change with temperature. In Figure 4, we plot the equilibrium market tightness as a function of temperature and wage, where the surface represents $\theta_T(w)$. We also present cross-sections at different wage levels in

Figure 4. Market Tightness

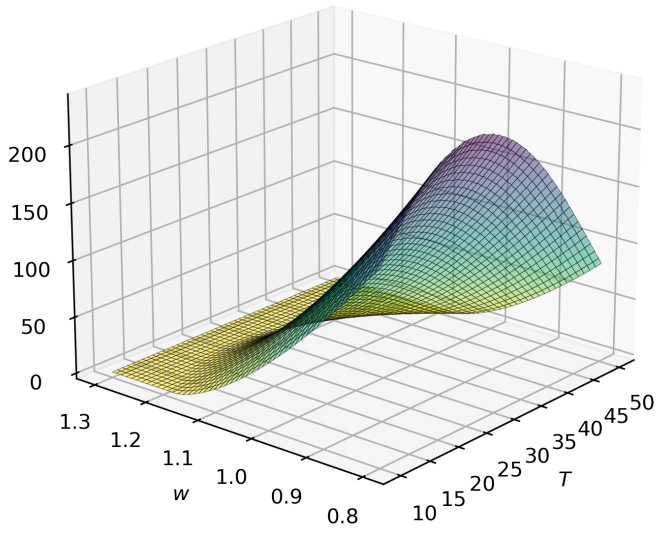

Notes: (a) This figure illustrates the equilibrium market tightness θ as a function of wage rate (w) and temperature (T). (b) On the surface plot, lower values indicate a tighter labor market, while higher values reflect more vacancies relative to unemployed workers.

Panel (a) of Figure 5. It can be observed that θ decreases with the wage rate, indicating a tighter market for high-paying jobs. This result is consistent with standard findings in direct search models. Regarding the effect of temperature, we find an inverse U-shaped relationship in market tightness. Starting from 10°C, θ increases with temperature, suggesting a rising vacancy-to-unemployment ratio. However, beyond a certain threshold, this ratio declines, indicating a tighter job market at higher temperatures. This occurs because firms anticipate a decline in workers' productivity under high temperatures. Consequently, the expected value of a job when hiring, i.e., $\mathbb{E}(J_T(z,w)|T,q=0)$ in Equation 15, decreases, leading to a reduction in market tightness θ. Furthermore, we find that the curvature for high-wage jobs (e.g., the dash-dot line in Panel (a) of Figure 5) is smaller than that for low-wage jobs (e.g., the solid line). This suggests that in our model, high-wage jobs are less sensitive to temperature variations.

Panel (b) of Figure 5 shows the optimal search behaviors of unemployed workers in the job market. The figure plots the optimal wage against temperature and wealth. Similar to market tightness, the optimal wage choice also exhibits an inverse U-shaped relationship with temperature, where w^* initially increases with temperature, peaks around moderate temperatures (approximately 25°C), and then declines at higher temperatures. This suggests that when the temperature exceeds a certain

threshold, workers direct their search toward lower-wage jobs. The underlying reason for this pattern is that firms reduce vacancy postings at higher temperatures, leading to a tighter labor market. In response, job seekers, facing a tighter labor market, would exhibit more risk-averse behavior by targeting lower-wage positions to increase their chances of employment.

Additionally, our model reveals the relationship between wealth and job search behavior. Poor individuals, particularly those facing asset constraints (solid line), tend to direct their search toward low-wage jobs. This finding is consistent with the notion that financial security enables greater selectivity in job searching, whereas individuals with limited assets exhibit more risk-averse behavior in the labor market.

Figure 5. Market Tightness and Optimal Wage

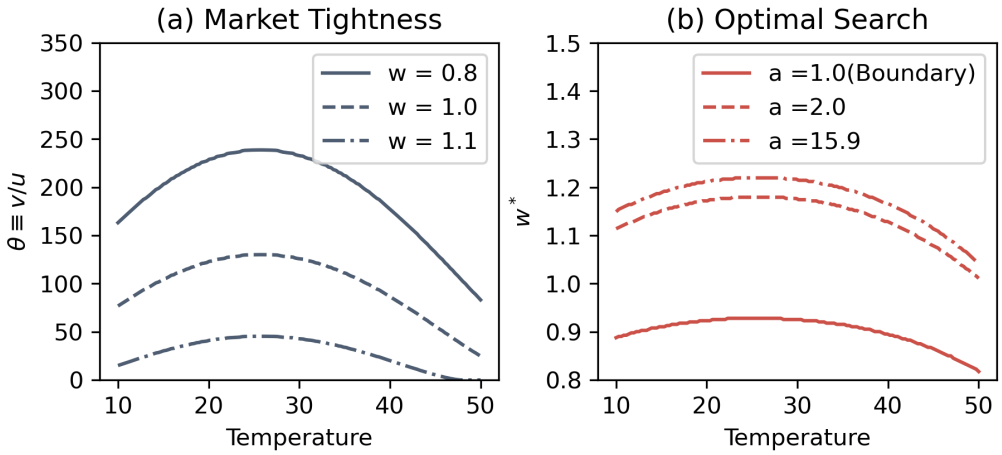

Notes: (a) Panel (a) illustrates the equilibrium market tightness $\theta = v/u$ as a function of temperature for different wage levels (w). (b) Panel (b) shows the optimal search wage w^* across temperatures for different wealth levels (a). The solid, dashed, and dash-dotted lines correspond to different levels of wealth.

VI. Aggregate Effects of Climate Change

A. Global Warming Scenario

We now evaluate the effect of temperature on inequality and other aggregate variables. As specified in the model setup, T is the state variable representing the population exposed to different temperature levels. In section II., we fitted the empirical distribution in Vietnam using the Bimodal distributions. For clarity, the term temperature distribution in our subsequent discussion specifically refers to the distribution of the population across different temperature levels.

To model the effects of climate change, we consider several scenarios. In the main text, we focus on the prominent phenomenon of global warming. As our first experiment, we assume that temperature follows a bimodal distribution as a

weighted sum of two normal distributions, i.e., the Bimodal-Normal distribution as in Equation 21. We begin with the parameters fitting the empirical data. Then, we vary the mean temperature from approximately 25°C to 30.5°C while holding the variance of the distribution fixed at the baseline level. We select 30.5°C based on the 60-year temperature projection from the HadGEM2 model under the RCP 8.5 scenario.[7] We assume the current average temperature is 25°C and project future temperatures over the next 60 years. Under the Lower Warming Projection (0.3°C per decade), the temperature reaches 27.7°C by 2085, while under the Higher Warming Projection (0.6°C per decade), it reaches 30.4°C by 2085. In Panel (a) of Figure 6, we depict several sample distributions for this experiment in different colors.

To analyze the impact under different assumptions about temperature distribution, we also simulate changes using a bimodal distribution composed of two log-normal distributions, i.e., the Bimodal-Lognormal distribution as in Equation 22. Similarly, we increase the average temperature from 25°C to 30.5°C, as in the previous experiment. The corresponding sample distribution is plotted in Panel (b) of Figure 6. It can be observed that, under the second experiment with a log-normal distribution, as the average temperature increases, the tail of the distribution thickens, implying a higher likelihood of extreme temperatures compared to the first experiment in Panel (a). In the following analysis, we will use Bimodal-Normal distribution and Bimodal-Log-normal distribution to denote distributions used in these two experiments.

As an alternative assumption for a sensitivity check, in Appendix B, we assume that the average temperature follows either a normal or a log-normal distribution. We plot the corresponding distribution paths in Figure B1.

[7]The RCP 8.5 scenario in the HadGEM2 climate model represents a high-emission Representative Concentration Pathway (RCP) used in climate projections.

Figure 6. Temperature Distribution Scenario (Bimodal Distributions)

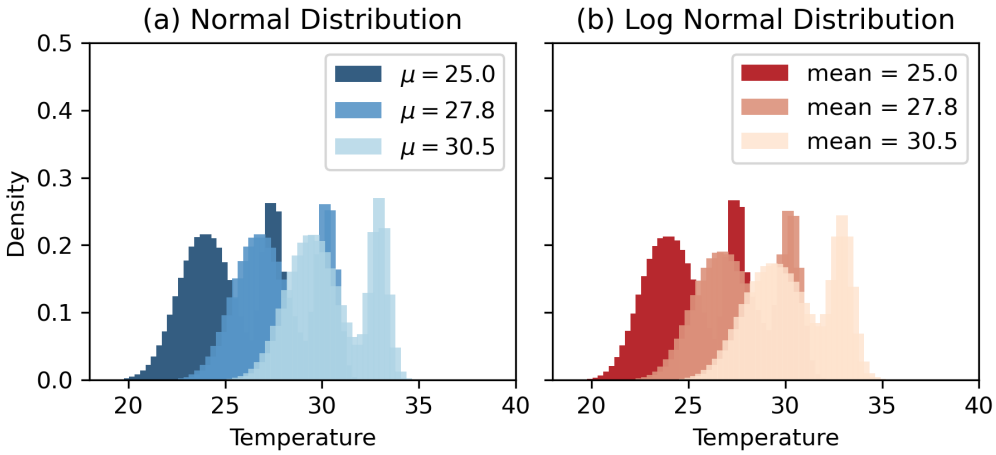

Notes: (a) This figure presents the sample distributions used for simulation in this section. (b) Panel (a) assumes that temperature follows a bimodal distribution with two normal distributions, $p_1\mathcal{N}(\mu_1, \sigma_1^2) + p_2\mathcal{N}(\mu_2, \sigma_2^2)$, with a fixed standard deviation of $\sigma_1 = 1.31, \sigma_2 = 0.44$ while varying the mean from 25 to 30.5. (c) Panel (b) assumes that temperature follows a Bimodal distribution with two log-normal distribution, $\mathbb{P} = p_1\text{LogN}(e^{\mu_1}, s_1) + p_2\text{LogN}(e^{\mu_2}, s_2)$, adjusting the scale parameter so that the mean temperature aligns with the corresponding normal distribution experiment.

We first present the benchmark results for the scenario in which temperature follows a Bimodal-Normal distribution, with an average temperature of approximately 25°C. Figure 7 plots the distributions of income and wealth in the stationary equilibrium. Panel (a) of the figure displays the distribution of instantaneous income, given by $ra + wz\mathbb{1}(q = 1)$. It could be viewed that in our model, income clusters in several groups. The disparity arises from multiple sources: unemployed workers cluster in the low-income range, while employed workers' incomes primarily vary based on their productivity levels. High-productivity workers concentrate in the high-income range, whereas low-productivity workers remain at lower income levels.

Furthermore, within each employment and productivity group, the income distribution exhibits positive skewness. This pattern arises due to capital income, which follows the positively skewed wealth distribution depicted in Panel (b). Such a wealth distribution is a common feature in heterogeneous-agent models. In our model, wealth disparity is driven not only by standard consumption-savings decisions but also by labor market frictions. The process of searching, hiring, and unemployment introduces additional heterogeneity, influencing individuals' wealth accumulation process.

In our model, the income Gini index is approximately 0.262, while the wealth Gini index is around 0.293. These measures provide a quantitative assessment of inequality in the economy. In the subsequent analysis, we will examine how these

disparities evolve under different temperature distributions, as plotted in Figure 6.

Figure 7. Benchmark Stationary Distribution

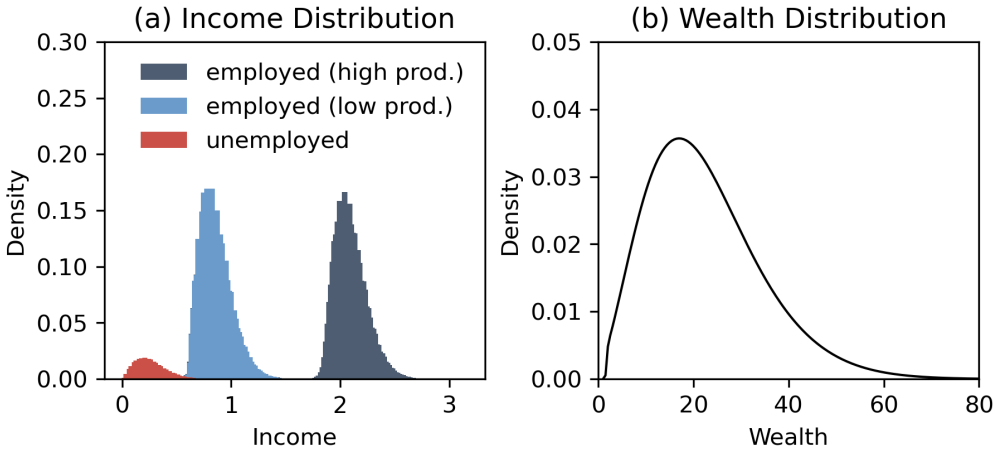

Notes: (a) This figure presents the stationary distribution under the benchmark temperature distribution with mean equals to 25°C. (b) Panel (a) depicts the distribution of instantaneous income. The black and blue bars represent the income distributions of employed workers with high and low productivity, respectively, while the red bars represent the income distribution of unemployed workers. (c) Panel (b) shows the stationary distribution of individual wealth a.

B. The Effects on Labor Market Outcomes

Table IV summarizes the labor market outcomes under different temperature distributions and scenarios. We present two typical scenarios in this table: an expected temperature of 25°C, which represents the average temperature in our data, and 30.5°C, which corresponds to the projected 60-year average temperature based on the HadGEM2 model. The first and second columns display the results under the assumption that temperature follows a Bimodal-Normal distribution and a Bimodal-Log-normal distribution, respectively. It can be observed that the labor market becomes more constrained at higher temperatures, with θ declining from 5.055 to 4.974, representing a 1.625% decrease under the Bimodal-Normal distribution. In the case of the Bimodal-Log-normal distribution, the effect is more pronounced, tightening the labor market by 1.704%.

Correspondingly, unemployed workers adjust their job search behavior by targeting lower-wage jobs. As shown in the second block of Table IV, the optimal wage threshold for job search declines from 1.213 to 1.206 (a 0.57% decrease) under the Bimodal-Normal distribution and from 1.213 to 1.205 (a 0.6% decrease) under the Bimodal-Log-normal distribution. This implies that as the average temperature rises, workers revise their expectations downward in response to increasing market tightness. This trend suggests a potential wage stagnation effect due to climate

change, where fewer job opportunities force workers to accept lower wages. Consequently, the equilibrium wage rate distribution shifts as the average temperature increases. We visualize the corresponding distribution in Figure 8. It can be observed that the distribution shifts leftward and becomes more dispersed when the average temperature rises to 30°C.

Figure 8. Wage Rate Distribution

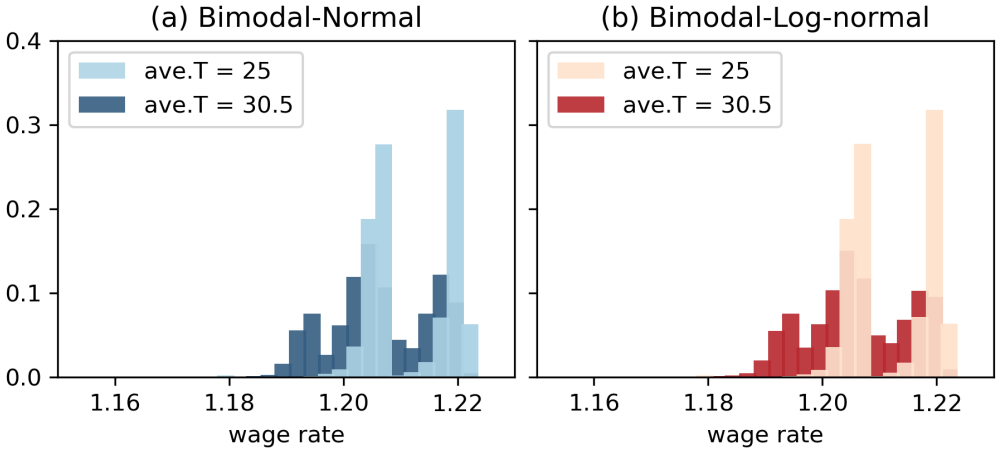

Notes: (a) This figure illustrates the stationary distribution of wage rates under different temperature scenarios. Panel (a) presents results for the Bimodal-Normal temperature distribution, while Panel (b) shows results for the Bimodal-Log-normal distribution. In both panels, the wage rate distributions are plotted for two expected temperature levels: $\mathbb{E}(T) = 25°C$ (lighter bars) and $\mathbb{E}(T) = 30.5°C$ (darker bars).

The unemployment rate also increases correspondingly as the labor market tightens due to higher average temperatures. In the third block of Table IV, our model indicates a 0.54% and 0.561% increase in the unemployment rate under the Bimodal-Normal and Bimodal-Log-normal distribution assumptions, respectively. To further visualize the impact of temperature on unemployment, we plot the stationary unemployment rate across different average temperature levels in Figure 9. It can be observed that unemployment increases with rising average temperatures. Moreover, the marginal increase in unemployment is more pronounced at higher temperatures, particularly when the average temperature exceeds 28°C. This indicates that not only does the overall unemployment rate rise due to global warming, but the marginal effect of temperature on unemployment also intensifies as temperatures increase.

Additionally, when comparing the effects on labor market outcomes under different assumptions about temperature distribution, we find that the magnitude of the impact is slightly greater when temperature follows a Bimodal-Log-normal distribution compared to a Bimodal-Normal distribution. This occurs because, in a positively skewed temperature distribution, a larger share of the population is exposed to higher-than-average temperatures, further tightening the labor market. In

Table IV. Labor Market in Different Scenarios

	(1) Bimodal-Normal	(2) Bimodal-Log-normal
Market Tightness θ		
$\mathbb{E}(T) = 24.8°C$	5.055	5.055
$\mathbb{E}(T) = 30.4°C$	4.974	4.97
Percentage Change (%)	-1.625	-1.704
Wage to Search w^*		
$\mathbb{E}(T) = 24.8°C$	1.213	1.213
$\mathbb{E}(T) = 30.4°C$	1.206	1.205
Percentage Change (%)	-0.577	-0.608
Unemployment Rate		
$\mathbb{E}(T) = 24.8°C$	4.877	4.877
$\mathbb{E}(T) = 30.4°C$	4.904	4.905
Percentage Change (%)	0.54	0.561

Notes: This table summarizes key labor market indicators under different temperature distributions. Column (1) presents results under a normal temperature distribution, while Column (2) corresponds to a log-normal distribution. For each scenario, we report market tightness (θ), the optimal wage to search (w^*), and the unemployment rate, evaluated at two different mean temperatures: $\mathbb{E}(T) = 24.8°C$ and $\mathbb{E}(T) = 30.4°C$. The percentage change reflects the relative difference between the two temperature levels.

contrast, under a Bimodal-normal temperature distribution, fewer individuals experience extreme heat, resulting in a relatively less pronounced effect on market tightness, job search behavior, and the unemployment rate.

Figure 9. Unemployment Change

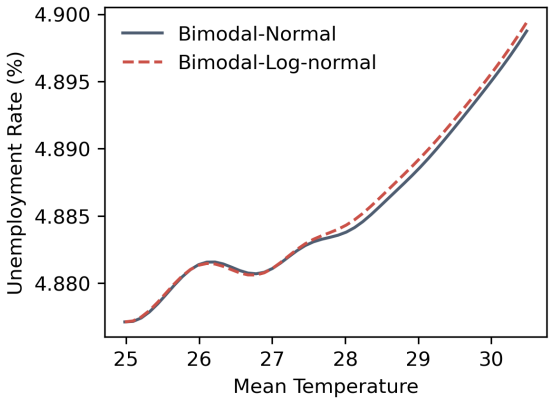

Notes: (a) This Figure shows the equilibrium unemployment rate as a function of mean temperature under two different temperature distributions: Bimodal-Normal (solid line) and Bimodal-Log-normal (dashed line). (b) The mean temperature varies from 25°C to 30.5°C.

In Appendix Table A2 and Figure B2, we conduct a similar analysis under the assumption that temperature follows a simple Normal or Log-normal distribution. We observe similar changes in searching and matching behavior, as well as in the aggregate unemployment rate. The labor market becomes tighter, and the unem-

ployment rate increases as the average temperature rises. Unlike the experiment in the main text, the difference between the Normal and Log-normal distributions is more pronounced than in the Bimodal distribution case.

C. The Effects on Income, Wealth and Inequality

We now begin examining the effects of temperature on aggregate income, wealth, and their respective distributions. Figure 10 illustrates the relationship between temperature and inequality, as measured by the Gini index for both income (Panel (a)) and wealth (Panel (b)).

In Panel (a), we observe that income disparity increases as the average temperature rises from approximately 25°C to over 30.5°C. This suggests that higher temperatures contribute to widening income inequality. Additionally, the effect is more pronounced under the Bimodal-Log-normal temperature distribution, which results in a slightly steeper increase in inequality. This reinforces the idea that a positively skewed temperature distribution exposes a larger share of the population to extreme heat, intensifying income disparities. Panel (b) presents a similar pattern for wealth inequality. The wealth Gini index exhibits a U-shaped pattern, initially decreasing with average temperature when temperatures are moderate and increasing once the average temperature exceeds a certain threshold. Furthermore, we observe that the change in the wealth Gini index is smaller than the change in the income Gini index. This discrepancy may be attributed to individuals' consumption-smoothing behavior, where precautionary savings help insure part of the income losses resulting from a tighter labor market and lower expected productivity. We will further our discussion on wealth inequality later in the next section.

Figure 10. Inequality Change

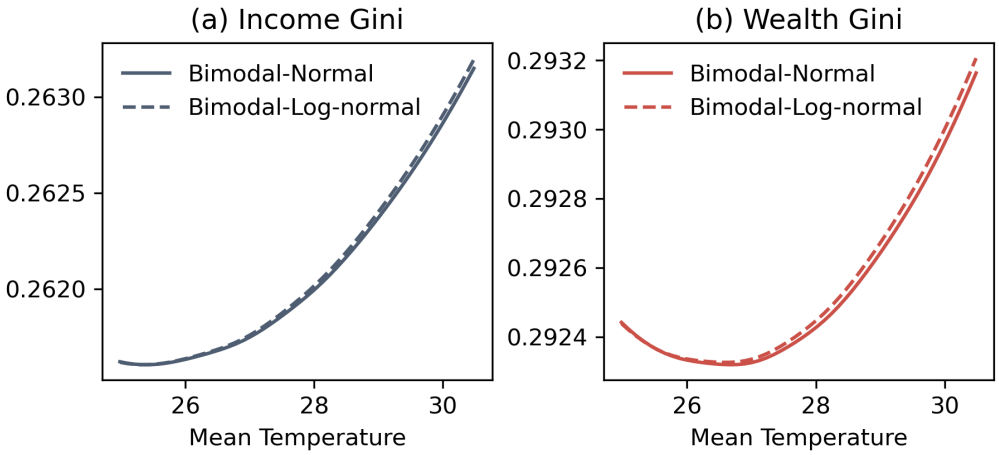

Notes: (a) This figure illustrates the changes in income inequality (Panel a) and wealth inequality (Panel b) as measured by the Gini index under different temperature distributions. (b) The solid and dashed lines represent results under the Bimodal-Normal and Bimodal-Log-normal temperature distribution assumptions, respectively.

Similar to the dynamics of unemployment, the increase in income and wealth inequality with rising temperatures also exhibits an increasing marginal effect. To further illustrate this, Figure 11 presents the marginal proportional change in aggregate income, wealth, and their respective Gini indices when the average temperature increases by 1°C. On one hand, aggregate income and wealth decline as the average temperature rises, with their marginal changes being negative and decreasing. On the other hand, the Gini indices for both income and wealth increase, with their marginal effects being positive and growing. This indicates that the negative effects of temperature on economic output, as well as econoic equality, intensify at higher temperatures. However, the difference in marginal effects between the Bimodal-Normal and Bimodal-Log-normal distributions is negligible.

To quantify these effects, Table V presents the predicted changes in economic outcomes under the assumption that temperature follows a Bimodal-Normal distribution. When the average temperature rises from 25°C to 30.5°C, mean income declines by 1.41% (from 1.43 to 1.41), while mean wealth decreases by 0.99% (from 22.56 to 22.34). However, despite these aggregate declines, inequality worsens. The income Gini index increases by 0.71%, and the wealth Gini index rises by around 0.33%. These findings highlight the main implication of climate change in our model: rising temperatures reduce average productivity, income, and wealth accumulation. However, the effects are not evenly distributed. Both income and wealth inequality worsen as a result. Furthermore, the impact exhibits an increasing marginal effect, meaning that as temperatures continue to rise, inequality intensifies at an accelerating rate.

Figure 11. The Effects on Income and Wealth

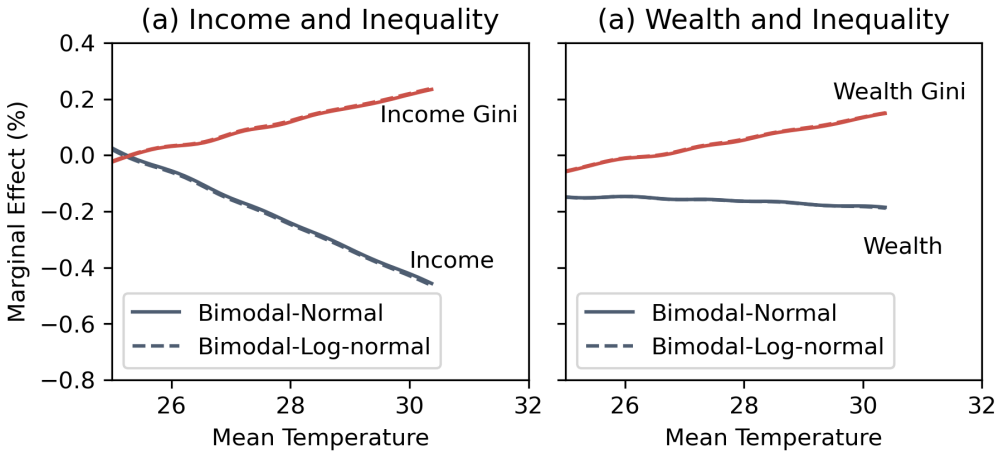

Notes: (a) This figure illustrates the marginal effect of a $1°C$ increase in average temperature. (b) Panel (a) presents the marginal effects of mean temperature on income and income inequality, measured by the Gini index. (c) Panel (b) shows the marginal effects of mean temperature on wealth and wealth inequality. Solid and dashed lines represent results under Bimodal-Normal and Bimodal-Log-normal temperature distribution assumptions, respectively.

Wealth Share: We further investigate wealth inequality by analyzing the distribution of wealth across different quantiles. As shown in rows 2 to 4 of the first block in Table V, the wealth share of the lowest 25% is approximately 10.2% under the baseline temperature distribution. However, as the average temperature increases to 30.5°C, this share declines by 0.29%. Similarly, the wealth shares of the second and third quantiles also decrease, though by a smaller margin of less than 0.1%. However, the wealthiest 25% experience a gain, with their share increasing by 0.17%, from 43.15% to 43.22%.

Income Disparities by Groups: Regarding income and income inequality, we present several statistics in the second block of Table V. As shown previously in Figure 10, heterogeneity in wealth, productivity, and employment status contributes to income disparity in our model. To identify the sources of rising income inequality, we calculate the average income across these dimensions of heterogeneity.

First, in lines 2 and 3 of the second block of Table IV, we observe that as the average temperature increases from 25°C to 30.5°C, the average income of both unemployed and employed workers declines. The magnitude of this income drop is larger for employed workers. This occurs because a decline in the average wage rate and productivity reduces labor income (wz) for employed workers. However, unemployed workers, who rely solely on capital income (ra), experience income reductions primarily due to wealth shrinkage. Consequently, the share of capital income in total income increases by approximately 0.41% during this transition,

as shown in the last row. As a result, the income gap between unemployed and employed workers narrows with rising average temperatures.

In contrast, income disparity across wealth and productivity levels widens. As shown in lines 4 to 8 of the second block of Table IV, the average income declines by 1.24% for individuals in the first quantile of the wealth distribution (poorest 25%), compared to 1.21% in the second and third quantiles and 1.12% in the wealthiest quantile. Income for the low-productivity group decreases from 0.831 to 0.825 (a drop of approximately 0.688%), while income for the high-productivity group declines from 2.019 to 2.007 (around 0.636%).

In Appendix Figure B3 and Table A3, we conduct the same analysis under the assumption that temperature follows a normal distribution. Average income, wealth, and their corresponding inequality measures change in the same direction as observed in our baseline experiment.

In summary, rising income inequality in our model is driven by two opposing effects. First, as the average temperature increases, the rising unemployment rate and declining labor income reduce the income gap between employed and unemployed workers. However, the widening income disparity across different wealth and productivity levels outweighs this effect, leading to an overall increase in income inequality.

D. Wealth Inequality and Consumption Saving Choice

In the previous section, we showed that our model predicts an increase in both income and wealth inequality under a global warming scenario. We also demonstrated that income inequality is primarily exacerbated by disparities across wealth levels and productivity groups. How does rising income inequality contribute to greater wealth inequality? To answer this question, we further analyze the mechanism driving the increase in the wealth Gini index.

First, income disparity across wealth levels could directly contribute to wealth inequality. As mentioned earlier, rising average temperatures affect income disproportionately across wealth levels, with wealthier individuals being less vulnerable. This is because wealthier people have higher share of capital income, which remains unaffected by temperature-induced declines in labor productivity and wage rates. Poorer individuals, who rely more on labor income, are more adversely affected.

However, whether higher income translates into higher wealth also depends on individuals' net savings. Thus, we extend our analysis by examining individuals' consumption-savings choices. We plot the policy function for consumption and savings in Appendix Figure B5. In the main text, we focus on the marginal propensity to consume (MPC). Following Achdou et al. (2022); Kaplan and Violante (2022), we compute the MPC in the HACT framework as follows.

Table V. Stationary Outcomes in Different Scenarios (Normal Distribution)

	(1) $25°C$	(2) $30.5°C$	(3) % Change
Wealth			
Mean	22.558	22.336	-0.991
Wealth Share			
0% - 25%	10.196	10.167	-0.285
25% - 75%	46.656	46.611	-0.095
75% - 100%	43.148	43.222	0.170
Gini	0.292	0.293	0.326
Income			
Mean	1.425	1.405	-1.412
Average by Employment			
Unemployed	0.264	0.262	-0.998
Employed	1.485	1.464	-1.393
Average by Wealth			
0% - 25%	1.154	1.140	-1.241
25% - 75%	1.417	1.400	-1.208
75% - 100%	1.686	1.667	-1.118
Average by Productivity			
Low Prod.	0.831	0.825	-0.688
High Prod.	2.019	2.007	-0.636
Gini	0.262	0.263	0.707
Capital Income Share	0.244	0.245	0.409

Notes: (a) This table presents stationary wealth and income outcomes under different mean temperature scenarios, assuming a Normal temperature distribution. Column (1) reports results for $\mathbb{E}(T) = 25°C$, while Column (2) shows results for $\mathbb{E}(T) = 30.5°C$. Column (3) reports the percentage change between the two scenarios. (b) Wealth outcomes include mean wealth, wealth distribution across percentiles, and the Gini coefficient. Income outcomes include mean income, capital income share, average income by wealth and productivity groups, and the income Gini coefficient.

First, we obtain expected total consumption over a given period τ as

$$C = \mathbb{E} \int_0^\tau c^* dt, \tag{23}$$

where c^* represents the optimal consumption function.[8] Then, defining an income realization of Δ, the MPC for wealth a and income Δ is given by

$$MPC(a, \Delta) = \frac{\mathbb{E}[C(a + \Delta)] - \mathbb{E}[C(a)]}{\Delta}, \tag{24}$$

where $\mathbb{E}[C(a)]$ denotes the expected consumption, aggregating all heterogeneities except for wealth. In practice, we set τ to 1 year and compute the MPC for each wealth percentile under $\Delta \in [0, 3]$.

We plot the corresponding results in Figure 12, where Panels (a) to (c) represent the MPC for individuals at the 10%, 50%, and 90% percentiles of the wealth distri-

[8] C can be obtained using the Feynman-Kac Formula.

bution, respectively, under different temperature distributions. Similar Figure but assuming normal distribution is plot in Figure B6. It can be observed that for poorer individuals (10% of wealth distribution), the difference in MPC between an average temperature of 25°C and 30.5°C is small. However, for individuals at the 50% percentiles of the wealth distribution, the MPC decreases slightly. Furthermore, at the 90% percentiles, the MPC declines with a larger proportional magnitude. We also plot the MPC under a scenario with higher temperature variance ($\sigma = 6.9$, depicted by the blue dotted line). The results indicate that wealthier individuals reduce their MPC even further compared to the baseline case with lower variance $\sigma = 4.2$.

Figure 12. Marginal Propensity to Consume

Notes: (a) This figure presents the annualized marginal propensity to consume (MPC) across different income realizations for individuals at different wealth percentiles. (b) Panels (a), (b), and (c) correspond to the 10th, 50th, and 90th percentiles of the wealth distribution, respectively. (c) The solid, dashed, and dotted lines represent different temperature distributions, with varying mean (μ) and standard deviation (σ), as indicated in the legend. (d) We assume temperature follows Binmodal-Normal distribution in this Figure.

How do the heterogeneous effects of rising average temperatures on income and MPC impact gross savings? We follow a similar approach as in Equation 23 to compute the expected savings over one year, given by

$$\mathbb{E}\int_0^\tau [ra + wz - c^*\mathbb{1}(q = 1)]dt, \tag{25}$$

for each wealth percentile. The corresponding results are plotted in Figure 13. Similar Figure but assuming normal distribution is plot in Figure B7. We observe distinct patterns between individuals in the lower wealth distribution (Panel (a)) and those in the higher wealth distribution (Panel (b)). As the average temperature increases from the baseline case to 30.5°C, savings for lower-wealth individuals remain nearly unchanged. However, we observe an increase in savings for individuals in the 80%-90% wealth percentile. This disparity is further amplified when we assume a higher variance with $\sigma = 6.9$.

Figure 13. Expected Savings in 1 Year

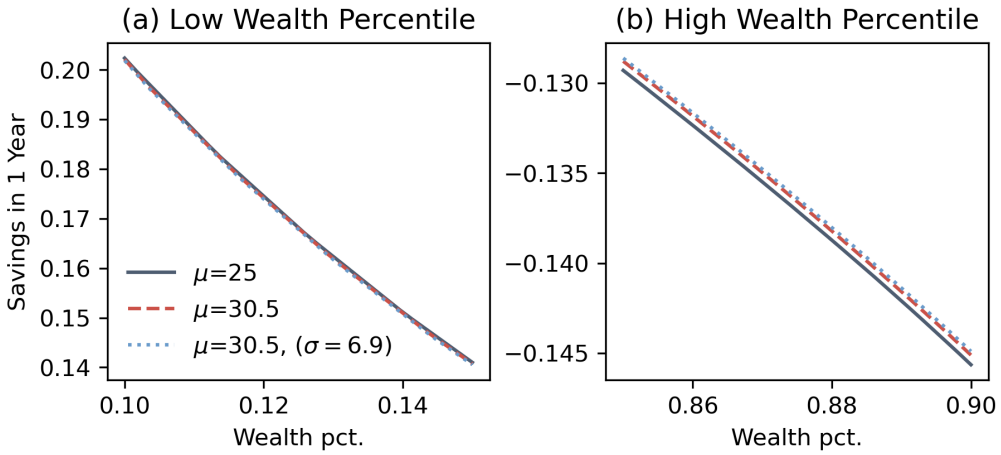

Notes: (a) This figure presents the annual savings rate across different wealth percentiles under varying temperature distributions. (b) Panel (a) shows the savings behavior for individuals in the lower wealth percentiles (10%–20%), while Panel (b) illustrates savings for those in the higher wealth percentiles (80%–90%). (c) The solid, dashed, and dotted lines correspond to different temperature distributions, characterized by varying mean (μ) and standard deviation (σ), as indicated in the legend.

In summary, the results in this section imply that in our model, global warming increase wealth disparities not only by disproportionately affecting instantaneous income but also through its impact on individuals' consumption-savings choices. Wealthier individuals are more precautionary in response to labor market and productivity risks induced by rising temperatures. As a result, they reduce their MPC more significantly and substitute more consumption for savings. In contrast, the MPC and net savings of lower-wealth individuals are less sensitive to temperature changes. Consequently, wealth accumulation occurs at a relatively faster rate for wealthier individuals, which worsen the wealth equality.

VII. Conclusions

This paper studies the impact of rising temperatures on labor market dynamics, productivity, and economic inequality through the lens of a structural equilibrium model. Motivated by empirical evidence from Vietnam, we develop a search-and-matching framework with heterogeneous agents, where productivity evolves as a two-state Markov process. The model endogenizes market tightness (θ) and equilibrium job search behavior, capturing how climate change affects labor markets and economic outcomes.

To quantify these effects, we estimate productivity transition probabilities using empirical data and map them into a continuous-time Poisson framework. We solve

the model using a combination of finite differencing methods for the Hamilton-Jacobi-Bellman (HJB) and Kolmogorov Forward (KF) equations, along with a fixed-point algorithm for computing equilibrium market tightness. This methodological approach allows us to link temperature variations to labor market frictions and firm hiring decisions.

Our results highlight an inverse U-shaped relationship between temperature and productivity, where moderate warming initially boosts output, but excessive heat leads to a sharp decline. Rising temperatures also tighten the labor market, as firms reduce hiring and workers adjust their job search strategies by targeting lower wages, contributing to wage stagnation. Moreover, temperature increases exacerbate income and wealth inequality, disproportionately affecting unemployed individuals who rely on capital income while high-productivity and wealthy workers remain more insulated from the effects of climate change.

This paper contributes to the literature by integrating climate economics and search-and-matching labor market theory, offering a novel equilibrium framework to study climate-induced labor market distortions. Our numerical solution approach - combining finite differencing for PDEs and fixed-point iteration for equilibrium conditions - provides a computationally efficient way to analyze these complex interactions. Future research could extend this framework to incorporate sectoral heterogeneity, adaptive labor market policies, and endogenous firm entry to further understand the long-term economic consequences of climate change.

References

Achdou, Yves, Jiequn Han, Jean-Michel Lasry, Pierre-Louis Lions, and Benjamin Moll. 2022. "Income and wealth distribution in macroeconomics: A continuous-time approach." The Review of Economic Studies, 89(1): 45–86.

Benhabib, Jess, Alberto Bisin, and Shenghao Zhu. 2015. "The wealth distribution in Bewley economies with capital income risk." Journal of Economic Theory, 159: 489–515.

Burke, Marshall, Solomon M Hsiang, and Edward Miguel. 2015. "Global non-linear effect of temperature on economic production." Nature, 527(7577): 235–239.

Carleton, Tamma A, and Solomon M Hsiang. 2016. "Social and economic impacts of climate." Science, 353(6304): aad9837.

Chaumont, Gaston, and Shouyong Shi. 2022. "Wealth accumulation, on-the-job search and inequality." Journal of Monetary Economics, 128: 51–71.

Dang, Hai-Anh H, Minh Cong Nguyen, and Trong-Anh Trinh. 2023. "Does hotter temperature increase poverty and inequality? Global evidence from subnational data analysis." WP 104, International Inequalities Institute, LSE.

Dang, Hai-Anh H, Stephane Hallegatte, and Trong-Anh Trinh. 2024. "Does global warming worsen poverty and inequality? An updated review." Journal of Economic Surveys, 38(5): 1873–1905.

Dell, Melissa, Benjamin F Jones, and Benjamin A Olken. 2012. "Temperature shocks and economic growth: Evidence from the last half century." American Economic Journal: Macroeconomics, 4(3): 66–95.

Diffenbaugh, Noah S, and Marshall Burke. 2019. "Global warming has increased global economic inequality." Proceedings of the National Academy of Sciences, 116(20): 9808–9813.

Eeckhout, Jan, and Alireza Sepahsalari. 2024. "The effect of wealth on worker productivity." Review of Economic Studies, 91(3): 1584–1633.

Espagne, Etienne, Thanh Ngo-Duc, Manh Hung Nguyen, Emmanuel Pannier, Marie-Noëlle Woillez, Alexis Drogoul, Thi Phuong Linh Huynh, Thuy Toan Le, Thi Thu Ha Nguyen, Truong Toan Nguyen, et al. 2021. "Climate change in Viet Nam; Impacts and adaptation. A COP26 assessment report of the GEMMES Viet Nam project." Paris AFD, 612.

Garg, Teevrat, Maulik Jagnani, and Vis Taraz. 2020. "Temperature and human capital in India." Journal of the Association of Environmental and Resource Economists, 7(6): 1113–1150.

Graff Zivin, Joshua, and Matthew Neidell. 2014. "Temperature and the allocation of time: Implications for climate change." Journal of Labor Economics, 32(1): 1–26.

Huggett, Mark. 1993. "The risk-free rate in heterogeneous-agent incomplete-insurance economies." Journal of economic Dynamics and Control, 17(5-6): 953–969.

Kaplan, Greg, and Giovanni L Violante. 2022. "The marginal propensity to consume in heterogeneous agent models." Annual Review of Economics, 14(1): 747–775.

Krusell, Per, and Anthony A Smith Jr. 2022. "Climate change around the world."

Krusell, Per, Jinfeng Luo, and Jose-Victor Rios-Rull. 2023. "Wealth, wages, and employment." Slides.

Nguyen, Cuong Viet, Manh-Hung Nguyen, and Toan Truong Nguyen. 2023. "The impact of cold waves and heat waves on mortality: Evidence from a lower middle-income country." Health Economics, 32(6): 1220–1243.

Office, General Statistics. 2018. "Report on Labor Force Survey." Ministry of Planning and Investment, Gov. Vietnam.

Somanathan, Eswaran, Rohini Somanathan, Anant Sudarshan, and Meenu Tewari. 2021. "The impact of temperature on productivity and labor supply: Evidence from Indian manufacturing." Journal of Political Economy, 129(6): 1797–1827.

Zander, Kerstin K, Wouter JW Botzen, Elspeth Oppermann, Tord Kjellstrom, and Stephen T Garnett. 2015. "Heat stress causes substantial labour productivity loss in Australia." Nature climate change, 5(7): 647–651.

Zhang, Peng, Olivier Deschenes, Kyle Meng, and Junjie Zhang. 2018. "Temperature effects on productivity and factor reallocation: Evidence from a half million Chinese manufacturing plants." Journal of Environmental Economics and Management, 88: 1–17.

Zhang, Xin, Xi Chen, and Xiaobo Zhang. 2024. "Temperature and low-stakes cognitive performance." Journal of the Association of Environmental and Resource Economists, 11(1): 75–96.

Zivin, Joshua Graff, Yingquan Song, Qu Tang, and Peng Zhang. 2020. "Temperature and high-stakes cognitive performance: Evidence from the national college entrance examination in China." Journal of Environmental Economics and Management, 104: 102365.

Appendices

A Tables

Table A1. Parameters to Fit the Empirical Temperature Distribution

	Bimodal-Normal	Bimodal-Log-normal
μ_1	23.97	24.01
μ_2	27.46	27.48
σ_1	1.31	0.06
σ_2	0.44	0.01
p_1	0.7	0.72
p_2	0.29	0.27

Notes: This table presents the estimated parameters for fitting the empirical temperature distribution using two different bimodal distributions: a sum of two normal distributions (Bimodal-Normal) and a sum of two log-normal distributions (Bimodal-Log-normal).

Table A2. Labour Market in Different Scenarios

	(1) Normal Dist.	(2) Log-normal Dist.
Market Tightness θ		
$\mathbb{E}(T) = 24.8°C$	5.006	4.984
$\mathbb{E}(T) = 30.4°C$	4.949	4.898
Percentage Change (%)	-1.152	-1.739
Wage to Search w^*		
$\mathbb{E}(T) = 24.8°C$	1.209	1.207
$\mathbb{E}(T) = 30.4°C$	1.203	1.198
Percentage Change (%)	-0.46	-0.713
Unemployment Rate		
$\mathbb{E}(T) = 24.8°C$	4.893	4.9
$\mathbb{E}(T) = 30.4°C$	4.911	4.927
Percentage Change (%)	0.365	0.556

Notes: This table summarizes key labour market indicators under different temperature distributions. Column (1) presents results under a normal temperature distribution, while Column (2) corresponds to a log-normal distribution. For each scenario, we report market tightness (θ), the optimal wage to search (w^*), and the unemployment rate, evaluated at two different mean temperatures: $\mathbb{E}(T) = 24.8°C$ and $\mathbb{E}(T) = 30.4°C$. The percentage change reflects the relative difference between the two temperature levels.

Table A3. Stationary Outcomes in Different Scenarios (Normal Distribution)

	(1) 24.8°C	(2) 30.4°C	(3) % Change
Wealth			
Mean	22.55	22.333	-0.969
Wealth Share			
0% - 25%	10.164	10.146	-0.176
25% - 75%	46.627	46.595	-0.067
75% - 100%	43.209	43.259	0.114
Gini	0.293	0.294	0.216
Income			
Mean	1.416	1.4	-1.13
Average by Employment			
Unemployed	0.264	0.262	-0.978
Employed	1.476	1.459	-1.116
Average by Wealth			
0% - 25%	1.146	1.135	-0.976
25% - 75%	1.408	1.395	-0.93
75% - 100%	1.677	1.662	-0.852
Average by Productivity			
Low Prod.	0.829	0.824	-0.612
High Prod.	2.014	2.004	-0.51
Gini	0.263	0.264	0.605
Capital Income Share	0.245	0.246	0.199

Notes: (a) This table presents stationary wealth and income outcomes under different mean temperature scenarios, assuming a normal temperature distribution. Column (1) reports results for $\mathbb{E}(T) = 24.8°C$, while Column (2) shows results for $\mathbb{E}(T) = 30.4°C$. Column (3) reports the percentage change between the two scenarios. (b) Wealth outcomes include mean wealth, wealth distribution across percentiles, and the Gini coefficient. Income outcomes include mean income, capital income share, average income by wealth and productivity groups, and the income Gini coefficient.

B Figures

Figure B1. Temperature Distribution Scenario (Normal and Lognormal)

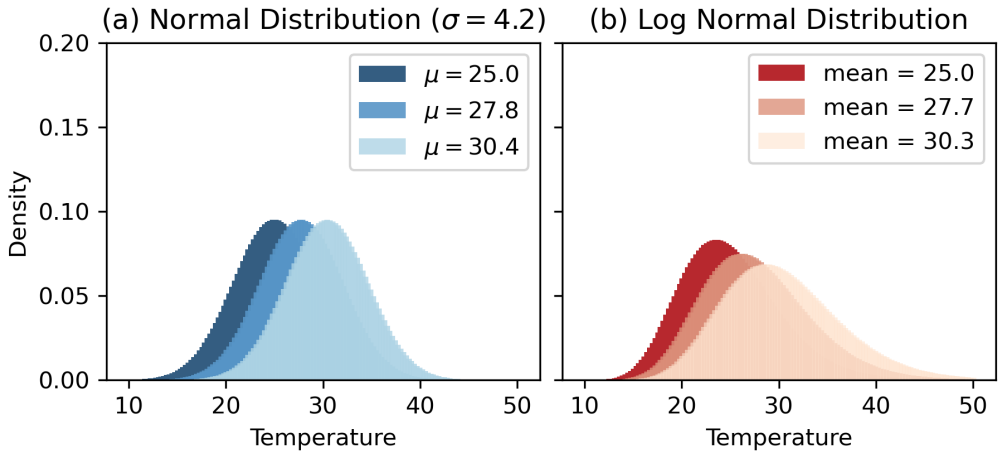

Notes: (a) This figure presents the sample distributions used for simulation in this section. (b) Panel (a) assumes that temperature follows a normal distribution, $\mathcal{N}(\mu, \sigma^2)$, with a fixed standard deviation of $\sigma = 4.2$ while varying the mean from 25 to 30.4. (c) Panel (b) assumes that temperature follows a log-normal distribution, adjusting the scale parameter so that the mean temperature aligns with the corresponding normal distribution experiment.

Figure B2. Unemployment Change

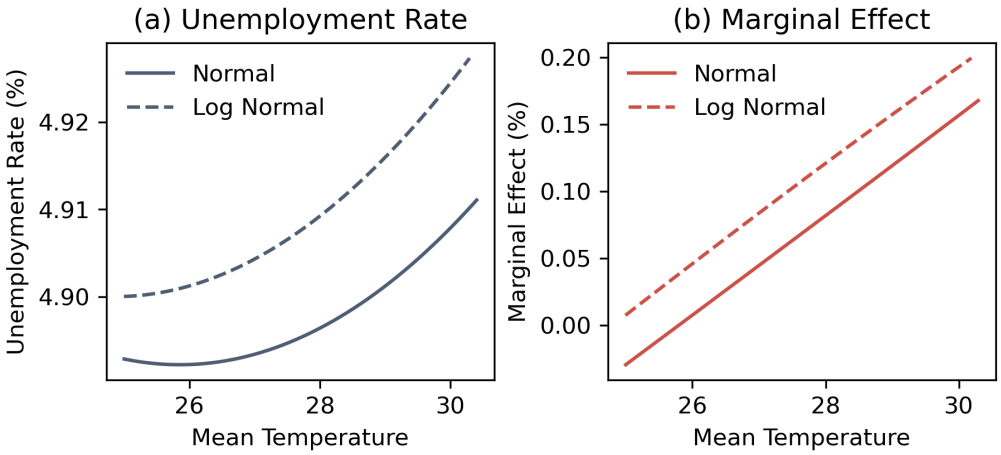

Notes: (a) Panel (a) shows the equilibrium unemployment rate as a function of mean temperature under two different temperature distributions: normal (solid line) and log-normal (dashed line). (b) Panel (b) presents the marginal effect of temperature on the unemployment rate, defined as the percentage change in unemployment when the average temperature increases by $1°C$.

Figure B3. Inequality Change

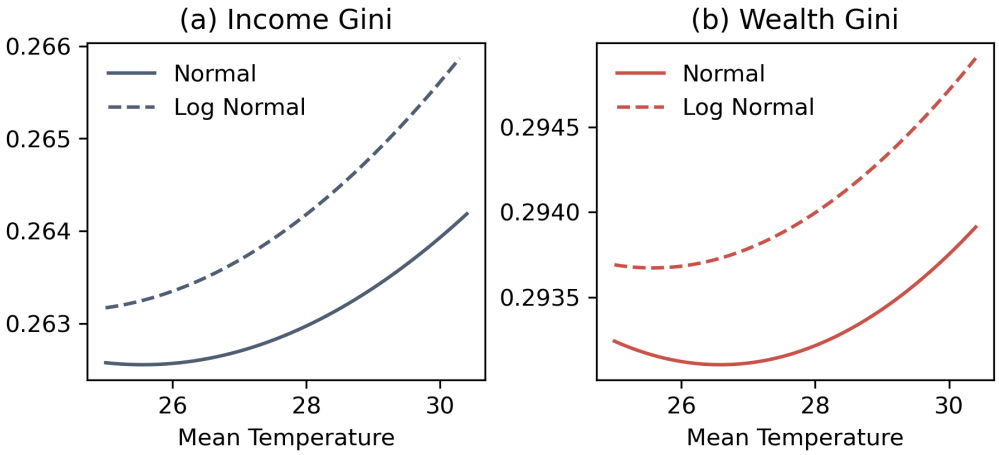

Notes: (a) This figure illustrates the changes in income inequality (Panel a) and wealth inequality (Panel b) as measured by the Gini index under different temperature distributions. (b) The solid and dashed lines represent results under the normal and log-normal temperature distribution assumptions, respectively.

Figure B4. The Effects on Income and Wealth

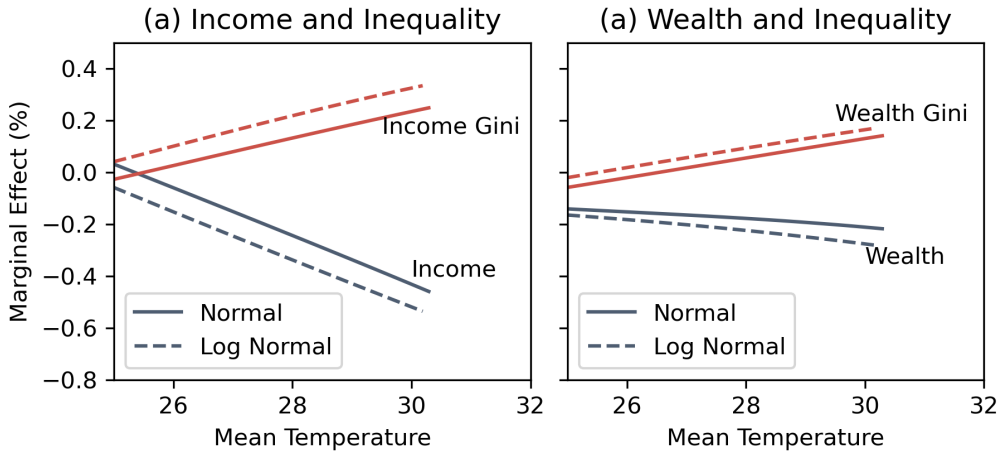

Notes: (a) This figure illustrates the marginal effect of a $1°C$ increase in average temperature. (b) Panel (a) presents the marginal effects of mean temperature on income and income inequality, measured by the Gini index. (c) Panel (b) shows the marginal effects of mean temperature on wealth and wealth inequality. Solid and dashed lines represent results under normal and log-normal temperature distribution assumptions, respectively.

Figure B5. Consumption Saving Policy Functions

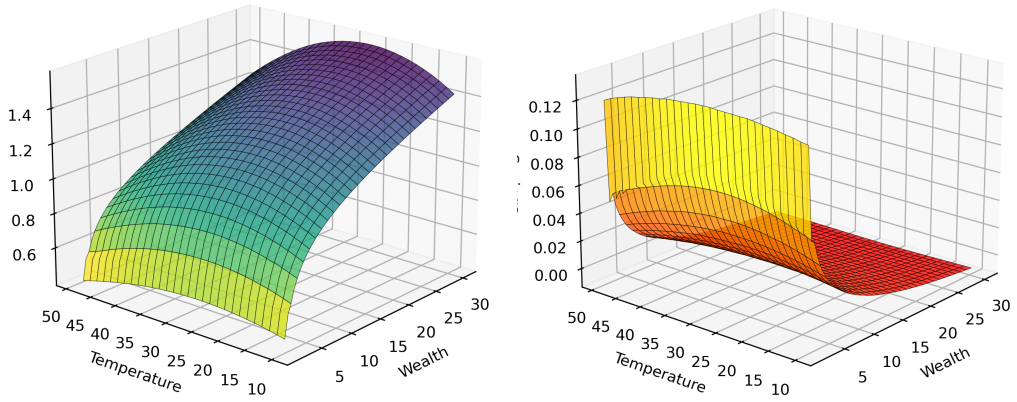

(a) Consumption **(b)** Savings

Figure B6. Marginal Propensity to Consume

Notes: (a) This figure presents the annualized marginal propensity to consume (MPC) across different income realizations for individuals at different wealth percentiles. (b) Panels (a), (b), and (c) correspond to the 10th, 50th, and 90th percentiles of the wealth distribution, respectively. (c) The solid, dashed, and dotted lines represent different temperature distributions, with varying mean (μ) and standard deviation (σ), as indicated in the legend. (d) We assume temperature follows normal distribution in this Figure.

Figure B7. Expected Savings in 1 Year

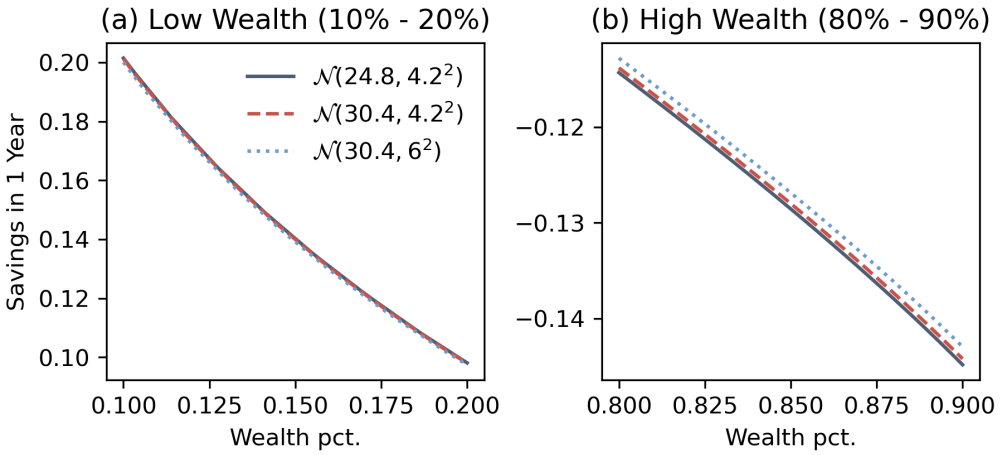

Notes: (a) This figure presents the annual savings rate across different wealth percentiles under varying temperature distributions. (b) Panel (a) shows the savings behaviour for individuals in the lower wealth percentiles (10%–20%), while Panel (b) illustrates savings for those in the higher wealth percentiles (80%–90%). (c) The solid, dashed, and dotted lines correspond to different temperature distributions, characterized by varying mean (μ) and standard deviation (σ), as indicated in the legend.

C Solution Method for the Structural Model

A. Worker's Problem

In this section, we rewrite the HJB equations in matrix form. Given a specific temperature T, the individual HJB includes four endogenous state variables: (a, z, w, q). We first stack the first three endogenous states, (a, z, w), and discretize the state space into finite grids, indexed by i, j, k.

At each time t and temperature T, we express the HJB equations using index notation as follows. For clarity, we omit subscripts t and T:

$$\begin{aligned}\rho E_{i,j,k} = \max_{c} \quad & u(c_{i,j,k}) + \frac{\partial E_{i,j,k}}{\partial a}[ra_i + w_k z_j - c_{i,j,k}] \\ & + \lambda_j[E_{i,j',k} - E_{i,j,k}] + \xi[U_{i,j} - E_{i,j,k}] + \frac{\partial E_{i,j,k}}{\partial t}.\end{aligned} \tag{C1}$$

$$\begin{aligned}\rho U_{i,j} = \max_{c,w} \quad & u(c_{i,j}) + \frac{\partial U_{i,j}}{\partial a}[ra_i - c_{i,j}] \\ & + \lambda_j[U_{i,j'} - U_{i,j}] + j(\theta_k)[E_{i,j,k} - U_{i,j}]^+ + \frac{\partial U_{i,j}}{\partial t}.\end{aligned} \tag{C2}$$

We first stack the asset dimension. By applying the finite differencing principle, we obtain

$$\begin{aligned}\frac{\partial E_{i,j,k}}{\partial a}[ra_i + w_k z_j - c_{i,j,k}] =& \frac{E_{i+1,j,k} - E_{i,j,k}}{da}\mu_a^+ + \frac{E_{i,j,k} - E_{i-1,j,k}}{da}\mu_a^- \\ =& \frac{\mu_a^+}{da}E_{i+1,j,k} + \frac{-\mu_a^+ + \mu_a^-}{da}E_{i,j,k} + \frac{\mu_a^-}{da}E_{i-1,j,k}.\end{aligned} \tag{C3}$$

Stacking the values as $\mathcal{E}_{j,k} = [E_{1,j,k}, E_{2,j,k}, \dots E_{na,j,k}]'$, we can express this in matrix form:

$$\frac{\partial E_{i,j,k}}{\partial a}[ra_i + w_k z_j - c_{i,j,k}] = \mathcal{A}_{j,k}\mathcal{E}_{j,k}, \tag{C4}$$

where

$$\mathcal{A}_{j,k} = \begin{bmatrix} \frac{-\mu_a^+ + \mu_a^-}{da} & \frac{\mu_a^-}{da} & 0 & \dots & 0 \\ \frac{\mu_a^+}{da} & \frac{-\mu_a^+ + \mu_a^-}{da} & \frac{\mu_a^-}{da} & \dots & 0 \\ 0 & \frac{\mu_a^+}{da} & \frac{-\mu_a^+ + \mu_a^-}{da} & \dots & 0 \\ \dots & \dots & \dots & \dots & \dots \\ 0 & 0 & 0 & \dots & \frac{-\mu_a^+ + \mu_a^-}{da} \end{bmatrix}. \tag{C5}$$

Next, we stack the productivity dimension j. Let $\mathbf{E}_k = [\mathcal{E}_{1,k}, \mathcal{E}_{2,k}]'$. Using the transition dynamics,

$$\lambda_j[E_{i,j',k} - E_{i,j,k}] = \begin{bmatrix} -\lambda_1 & \lambda_1 \\ \lambda_2 & -\lambda_2 \end{bmatrix} \begin{bmatrix} \mathcal{E}_{1,k} \\ \mathcal{E}_{2,k} \end{bmatrix}. \tag{C6}$$

Thus, the first two drift components in Equation C1 can be written as

$$\begin{bmatrix} \mathcal{A}_{1,k} - \lambda_1 & \lambda_1 \\ \lambda_2 & \mathcal{A}_{2,k} - \lambda_2 \end{bmatrix} \begin{bmatrix} \mathcal{E}_{1,k} \\ \mathcal{E}_{2,k} \end{bmatrix} \equiv \mathcal{B}_k \mathbf{E}_k. \tag{C7}$$

Similarly, stacking the wage and employment status dimensions, we can express the full system in matrix form:

$$\begin{bmatrix} \mathcal{B}_1 & 0 & 0 & \dots & 0 & 0 \\ 0 & \mathcal{B}_2 & 0 & \dots & 0 & 0 \\ \dots & \dots & \dots & \dots & \dots & \dots \\ 0 & 0 & 0 & \dots & \mathcal{B}_{nw} & 0 \\ 0 & 0 & 0 & \dots & 0 & \mathcal{B}_U \end{bmatrix} \begin{bmatrix} \mathbf{E}_1 \\ \mathbf{E}_2 \\ \dots \\ \mathbf{E}_{nw} \\ \mathbf{U} \end{bmatrix} \equiv \mathcal{C}\mathbf{V}. \tag{C8}$$

The transition matrix for job status is given by

$$\mathcal{T} = \begin{bmatrix} -\xi & 0 & \dots & 0 & \xi \\ 0 & -\xi & \dots & 0 & \xi \\ \dots & \dots & \dots & \dots & \dots \\ j(\theta_1)I_1 & j(\theta_2)I_2 & \dots & j(\theta_{nw})I_{nw} & \sum_k [j(\theta_k)I_k] \end{bmatrix}, \tag{C9}$$

where $I_k = \mathbb{1}(w^* = w_k)\mathbb{1}(E_{i,j,k} > U_{i,j})$. The HJB equations can thus be expressed as

$$\begin{aligned} \rho\mathbf{V} &= \mathbf{uc} + [\mathcal{C} + \mathcal{T}]\mathbf{V} + \frac{\partial}{\partial t}\mathbf{V} \\ &\equiv \mathbf{uc} + \Omega(\mathbf{V})\mathbf{V} + \frac{\partial}{\partial t}\mathbf{V}, \end{aligned} \tag{C10}$$

where we express the matrix Ω as a function of the value function $\mathbf{V}$. This is because Ω contains the optimal controls for consumption ($c^*_{i,j,k}$) and the optimal wage to search for ($w^*_{i,j}$), both of which are functions of the value function, as shown in **??**.

The associated Kolmogorov Forward Equation is:

$$\frac{\partial}{\partial t}\mathbf{G} = \Omega^*(\mathbf{V})\mathbf{G}, \tag{C11}$$

where Ω^* is the adjoint matrix of Ω.

B. *Worker's Problem*

Similar to the individual HJB, given that the value of a vacancy is zero, we discretize the job's value function as:

$$\rho^{\mathtt{f}} \mathcal{J}_{j,k} = \Pi_{j,k} - \xi \mathcal{J}_{j,k} + \lambda_j [\mathcal{J}_{j',k} - \mathcal{J}_{j,k}] + \frac{\partial \mathcal{J}}{\partial t}. \tag{C12}$$

Following a similar derivation as in the individual HJB, we rewrite the system in matrix form:

$$\rho^{\mathtt{f}} \begin{bmatrix} \mathcal{J}_{1,k} \\ \mathcal{J}_{2,k} \end{bmatrix} = \begin{bmatrix} \Pi_{1,k} \\ \Pi_{2,k} \end{bmatrix} - \xi \begin{bmatrix} \mathcal{J}_{1,k} \\ \mathcal{J}_{2,k} \end{bmatrix} + \begin{bmatrix} -\lambda_1 & \lambda_1 \\ \lambda_2 & -\lambda_2 \end{bmatrix} \begin{bmatrix} \mathcal{J}_{1,k} \\ \mathcal{J}_{2,k} \end{bmatrix}. \tag{C13}$$

Thus, we obtain:

$$(\rho^{\mathtt{f}} + \xi) \mathcal{J}_k = \Pi_k + \Lambda \mathcal{J}_k. \tag{C14}$$

Stacking over all wage levels k, we derive the final matrix representation:

$$(\rho^{\mathtt{f}} + \xi) \mathbf{J} = \Pi + \Lambda \mathbf{J} + \frac{\partial \mathbf{J}}{\partial t}. \tag{C15}$$

C. *Solving the Model*

Finite Differencing Method for PDEs. The system of PDEs (Equation C10, Equation C11, and Equation C15) can be solved using the implicit update method, as described in Achdou et al. (2022).

By further discretizing the time dimension t, Equation C10 can be rewritten as:

$$\begin{aligned} \frac{\mathbf{V}_{t+1} - \mathbf{V}_t}{\Delta} + \rho \mathbf{V}_{t+1} &= \mathbf{u} + \Omega(\mathbf{V}_t) \mathbf{V}_{t+1}, \\ \left((\rho + \frac{1}{\Delta}) I - \Omega(\mathbf{V}_t) \right) \mathbf{V}_{t+1} &= \mathbf{u} + \frac{\mathbf{V}_t}{\Delta}, \\ \mathbf{V}_{t+1} &= \left((\rho + \frac{1}{\Delta}) I - \Omega(\mathbf{V}_t) \right)^{-1} \frac{\mathbf{V}_t}{\Delta}. \end{aligned} \tag{C16}$$

In the stationary steady state, we have $\partial_t \mathbf{V}_t = 0$, implying that $\mathbf{V}_{t+1} = \mathbf{V}_t$. Therefore, we solve the HJB equation in the stationary equilibrium using the following approach: (1) Initialize $\mathbf{V}_0$ with an initial guess. (2) Iterate $\mathbf{V}_{t+1}$ using Equation C16 until $|\mathbf{V}_{t+1} - \mathbf{V}_t|$ is sufficiently small. (3) The converged value function, denoted as $\mathbf{V}_\infty$, represents the stationary equilibrium.

Using the value function $\mathbf{V}_\infty$ and the stationary equilibrium condition $\partial_t \mathbf{G}_t = 0$, we obtain:

$$0 = \Omega^*(\mathbf{V}_\infty)\mathbf{G}, \tag{C17}$$

from which we solve for the stationary distribution $\mathbf{G}_\infty$.

Applying the same iterative method, we also solve for the value function of jobs in the stationary equilibrium, denoted as $\mathbf{J}_\infty$.

Finding the Equilibrium Market Tightness θ. In our model, market tightness θ is an equilibrium object that varies across different average temperatures and wage levels. It is determined such that the market-clearing condition is satisfied. Given a specific average temperature T, market tightness as a function of wage w is expressed as:

$$\theta_T(w) = f^{-1}\left(\frac{\kappa}{\mathbb{E}[J_T(z,w)|T, q=0]}\right). \tag{C18}$$

where the denominator represents the conditional expectation of job value, given temperature and labor market conditions. Given the two-state process of productivity z, the expectation term can be written as:

$$\begin{aligned}\mathbb{E}[J_T(z,w)|T, q=0] = \mathbb{P}(z_1|T, q=0)J_T(z_1, w) \\ + \mathbb{P}(z_2|T, q=0)J_T(z_2, w),\end{aligned} \tag{C19}$$

where $\mathbb{P}(z_1|T, q=0)$ and $\mathbb{P}(z_2|T, q=0)$ denote the probabilities of an unemployed worker being in the high-productivity and low-productivity states, respectively, given a specific temperature T. This term is an endogenous equilibrium object since the unemployment rate $\mathbb{P}(q=0)$ is determined by market tightness θ.

Given these structures, we adopt a fixed-point algorithm to solve for equilibrium market tightness:

1. Initialize market tightness $\theta_T^{(0)}(w)$.

2. Given θ, solve the equilibrium HJB functions for individuals, $\mathbf{V}_\infty$, and for jobs, $\mathbf{J}_\infty$, following the steps introduced in this section.

3. Compute the corresponding probability distributions given $\theta_T^{(0)}(w)$, i.e., $\mathbb{P}(z_1|T, q=0; \theta_T^{(0)}(w))$ and $\mathbb{P}(z_2|T, q=0; \theta_T^{(0)}(w))$.

4. Calculate the expected value of jobs, $\mathbb{E}[J_T(z,w)|T, q=0; \theta_T^{(0)}(w)]$, and update market tightness using Equation C18. The updated tightness $\hat{\theta}_T(w)$ is given by:

$$\hat{\theta}_T(w) = f^{-1}\left(\frac{\kappa}{\mathbb{E}[J_T(z,w)|T, q=0; \theta_T^{(0)}(w)]}\right). \tag{C20}$$

5. Define a relaxation parameter ϕ, and update the market tightness for the next iteration:

$$\theta_T^{(1)}(w) = \phi\hat{\theta}_T(w) + (1-\phi)\theta_T^{(0)}(w). \tag{C21}$$

6. Iterate until the change in market tightness is sufficiently small:

$$|\theta_T^{(N)}(w) - \theta_T^{(N-1)}(w)| < \delta. \tag{C22}$$